REPORT DOCUMENTATION PAGE

1a. REPORT SECURITY CLASSIFICATION Unclassified	1b. RESTRICTIVE MARKINGS None
2a. SECURITY CLASSIFICATION AUTHORITY 2b. DECLASSIFICATION/DOWNGRADING SCHEDULE	3. DISTRIBUTION/AVAILABILITY OF REPORT Approved for public release; distribution is unlimited.
4. PERFORMING ORGANIZATION REPORT NUMBER(S) NORDA Report 178	5. MONITORING ORGANIZATION REPORT NUMBER(S) NORDA Report 178
6. NAME OF PERFORMING ORGANIZATION Naval Ocean Research and Development Activity	7a. NAME OF MONITORING ORGANIZATION Naval Ocean Research and Development Activity
6c. ADDRESS *(City, State, and ZIP Code)* Ocean Acoustics and Technology Directorate NSTL, Mississippi 39529-5004	7b. ADDRESS *(City, State, and ZIP Code)* Ocean Acoustics and Technology Directorate NSTL, Mississippi 39529-5004
8a. NAME OF FUNDING/SPONSORING ORGANIZATION Naval Ocean Research and Development Activity 8b. OFFICE SYMBOL *(If applicable)*	9. PROCUREMENT INSTRUMENT IDENTIFICATION NUMBER
8c. ADDRESS *(City, State, and ZIP Code)* Ocean Acoustics and Technology Directorate NSTL, Mississippi 39529-5004	10. SOURCE OF FUNDING NOS. PROGRAM ELEMENT NO. 65862N / PROJECT NO. / TASK NO. / WORK UNIT NO.
11. TITLE *(Include Security Classification)* High-Frequency Acoustic Bottom Scattering Experiments	
12. PERSONAL AUTHOR(S) S. Stanic, P. Fleischer, K. Briggs, M. Richardson, B. Eckstein	
13a. TYPE OF REPORT Final	13b. TIME COVERED From _____ To _____
14. DATE OF REPORT *(Yr., Mo., Day)* January 1987	15. PAGE COUNT 50
16. SUPPLEMENTARY NOTATION	
17. COSATI CODES FIELD / GROUP / SUB. GR.	18. SUBJECT TERMS *(Continue on reverse if necessary and identify by block number)* acoustics, reverberation, frequency, shallow water

19. ABSTRACT *(Continue on reverse if necessary and identify by block number)*

NORDA has established an environmental acoustics program that focuses on the relationships between ocean bottom physical properties and acoustic scattering. The program is designed to make environmentally supported acoustic scattering measurements in areas that range from simple and uniform to those that are more complex. With careful site selection it should be possible to correlate changes in ocean bottom physical properties with changes in acoustic scattering strength, correlation and coherence estimates.

Using expertise available in the Louisiana offshore oil industry, NORDA and PetroMarine, Inc.

20. DISTRIBUTION/AVAILABILITY OF ABSTRACT UNCLASSIFIED/UNLIMITED ☐ SAME AS RPT. ■ DTIC USERS ☐	21. ABSTRACT SECURITY CLASSIFICATION Unclassified	
22a. NAME OF RESPONSIBLE INDIVIDUAL J. Stephen Stanic	22b. TELEPHONE NUMBER *(Include Area Code)* (601) 688-5235	22c. OFFICE SYMBOL Code 243

Naval Ocean Research and Development Activity
January 1987
(NORDA – Report 178)

High-Frequency Acoustic Bottom Scattering Experiments, Part I: Instrumentation and Methods

S. Stanic
Ocean Acoustics Division
Ocean Acoustics and Technology Directorate

P. Fleischer
Seafloor Geosciences Division
Ocean Sciences Directorate

K. B. Briggs
M. D. Richardson
Oceanography Division
Ocean Sciences Directorate

B. Eckstein
Ocean Technology Division
Ocean Acoustics and Technology Directorate

Foreword

Many of the new concepts for torpedo guidance and control, minehunting and mine classification systems require a far more sophisticated knowledge of acoustic properties of the ocean boundaries than is presently used by systems in the Fleet. In order to address this issue, it is necessary to know the temporal and spatial coherence and variability of high-frequency acoustic energy both forward- and backscattered from the boundaries. Unfortunately, a reference data base describing these parameters is not available or is very limited. Furthermore, the instrumentation and the platforms to carry out high-frequency acoustic correlation experiments over a wide frequency range was not available until now.

This report outlines a program that focuses on the interaction of high-frequency acoustic energy with the ocean bottom. Specialized high-resolution acoustic and environmental measurement systems are used to investigate acoustic scattering from different ocean bottoms. Data collected in this manner will be destined to serve as inputs to present and future environmental acoustic scattering models.

A. C. Esau, Captain, USN
Commanding Officer, NORDA

Executive summary

NORDA has established an environmental acoustics program that focuses on the relationships between ocean-bottom physical properties and acoustic scattering. The program is designed to make environmentally supported acoustic scattering measurements in areas that range from simple and uniform to those that are more complex. With careful site selection it should be possible to correlate changes in ocean-bottom physical properties with changes in acoustic scattering strength, correlation and coherence estimates.

Using expertise available in the Louisiana offshore oil industry, NORDA and PetroMarine, Inc. designed and constructed two state-of-the-art shallow-water acoustic instrumentation support towers. The towers are designed to be transported to an experiment staging area, where they are then assembled and the instrumentation installed. Each tower is towed to a preselected site and deployed on the ocean bottom. Cables from each of the towers are attached to transmitting and receiving equipment located on a moored support ship.

The transmitting system consists of two nonlinear parametric sources with 2° beamwidth and source levels between 187 and 214 dB/μPa. The acoustic receiving systems utilize a pair of two-dimensional multielement spatial receiving arrays with broadband capabilities to 200 kHz.

Two experiments have been conducted in shallow-water sandy environments off the Florida coasts. The first experiment was in an area 19 miles south of Panama City, Florida. The second was located 26 miles east of Jacksonville, Florida. Each of these experiment sites was selected after extensive surveying. Environmental data were provided by sidescan survey imagery, stereophotography, and sediment analysis of diver-collected cores.

The large-scale environmental measurements and pre-site surveys used 3.5-kHz subbottom and 200-kHz bathymetry systems with a Klein 100-kHz sidescan sonar system. Precise navigation was provided by Loran C or Motorola miniranger systems. The general orientation of the experiment and tower placement was determined from sidescan sonar mosaics. Bathymetry data provided three-dimensional displays of large-scale features of the ocean bottom. Underwater color video camera coverage was employed to survey small-scale variability of the experiment areas.

Sediment and surface roughness measurements were used to classify each experiment site. Diver-collected sediment cores provided data on the geoacoustic properties of bottom sediments. Small-scale roughness estimates were obtained from analysis of a large number of stereophotographs.

Acoustic data analysis will provide estimates of scattering strength envelope statistics, correlation and coherence as a function of frequency, pulse length, grazing angle, azimuthal angle and environmental structure. Correlation of acoustic and environmental data will enable a critical evaluation of existing environmental acoustic models and generate new ideas in model development.

Acknowledgments

The authors particularly thank L. Carlton and W. Clay at the Naval Underwater Systems Center, New London, Connecticut, for development of the parametric acoustic sources used in the experiments. We also thank R. Love, D. Young, C. Levenson, R. Ray, B. Williams, B. Sawyer, N. Lombard, C. Watkins, and A. Kramer at NORDA, without whose contribution to the High-Frequency Shallow-Water Program, this project would have been impossible. We thank P. Blanchard and D. Sherman at PetroMarine Engineering, Gretna, Louisiana, for development of the acoustic towers. Thanks are due to the Naval Coastal Systems Center, Panama City, Florida, for cooperation with logistics and support for staging and testing. This work was supported by Office of Naval Research, Program Element 61153N, through the NORDA Defense Research Sciences Program, Dr. H. Eppert, Program Manager. Funds for design and construction of the acoustic towers were derived from Program Element 65862N.

Contents

High-frequency acoustic bottom scattering experiments: Part I: Instrumentation and methods

I. Introduction

In general, the acoustic characteristics of signals, noise, and reverberation in the deep ocean are significantly different from those in shallow or narrow coastal areas. The proximity of the boundaries, increased substrate and water-column inhomogeneity, and increased density or influence of noise sources contribute to the extreme complexity of the shallow-water acoustic environment. To develop naval systems that can operate effectively in shallow water, the interaction of environmental and acoustic parameters must be obtained and understood.

Over the past several decades considerable effort has been dedicated to understanding the effects of shallow-water, high-frequency ocean boundary scattering (Urick, 1975; Wong and Chesterman, 1968; McKinney and Anderson, 1964). Early measurements were obtained by using sources and receiving hydrophones that were hung over sides of research ships. These results were always contaminated by ship and source-receiver motions.

Recent measurements have been made using transducers mounted on tripod-like structures placed on the ocean bottom and hardwired to a support ship or research tower (Boehme et al., 1985). While source-receiver motions were eliminated, these instrumentation systems can be deployed only in calm seas using ships with moderate capacity cranes.

II. NORDA's high-frequency shallow-water program

A. Program objectives

Since the bottom is a major factor in the shallow-water environment, NORDA has established a program that focuses on the relationships between ocean-bottom properties and acoustic scattering. The program consists of an integrated series of acoustic and environmental measurements designed to identify and isolate various bottom-scattering mechanisms, and to resolve their effects on acoustic back- and forward-scattered fields. Data from these measurements will serve as a basis for developing shallow-water environmental acoustic models for use in exploratory and advanced development programs.

B. Scope

The relationships between the acoustic and geological experiments are outlined in Figure 1. This program concentrates on measuring acoustic boundary scattering from medium sand bottoms where roughness is determined by sand waves or by a coarse shell hash surficial layer. These regions are typical of those found along the East and Gulf Coasts. Two field experiments have been conducted. The first was located 19 miles south of Panama City, Florida, in 100 ft of water. This site was selected because of its homogeneous bottom properties, low shell content, and lack of significant roughness. This site is now serving as the site with which all others will be compared.

A second experiment has been conducted off the coast of Jacksonville, Florida. This area was more complex, and bottom roughness was determined by coarse shell. A third experiment is planned in an area where the roughness is due entirely to migrating sand waves. This experiment will take place in August 1987, 25 miles south of Panama City, Florida. By carefully selecting these experimental areas, it should be possible to correlate changes in the scattered acoustic signal characteristics with changes in bottom parameters.

The major technical objectives are to

- identify which geological, geoacoustic and geotechnical properties are relevant to the prediction of acoustic bottom scattering;
- determine the spatial and temporal variabilities of these parameters and to what extent these variations significantly affect acoustic scattering measurements;
- measure the statistics of acoustic reverberant and forward-scattered fields as a function of grazing angles, frequency, pulse length, and environmental parameters;
- determine the predictability of acoustic bottom scattering given the relevant geological and oceanographic parameters;
- experimentally determine the range of applicability of current scattering models;
- develop new models based on the application of the second-born approximations.

III. Acoustic instrumentation systems

A. Tower design

A major accomplishment of the program was the development of a new and novel method of deploying acoustic instrumentation on the ocean bottom. Using expertise available in the Louisiana offshore oil industry, NORDA and PetroMarine Engineering of Gretna, Louisiana, designed and constructed two state-of-the-art, shallow-water acoustic instrumentation systems (Fig. 2).

Each tower is a twin-hull catamaran design with a 60-inch-diameter vertical tank supporting an instrument chamber, a triaxial positioning system and a two-dimensional array mount. The array mount is a rigid tubular support structure for acoustic sources and receiving hydrophones. The sources and receiving arrays are aimed using the remotely controlled triaxial positioner. Each tower can be disassembled for transportation to an experimental staging area. The major subassemblies are shown in Figure 3.

The pontoons are 35 feet long and 48 inches in diameter. The center section of each pontoon is a sealed buoyancy chamber that is structurally reinforced by two watertight bulkheads. These chambers form part of the subsurface buoyancy system.

The two pontoons are connected by a sealed bridge structure that is 22 feet long and 7 feet wide, and is constructed from 12-inch-diameter steel pipe. The fourth major subassembly is a 12-foot-high, 60-inch-diameter vertical tank section. The upper 8 feet is a sealed buoyancy chamber and the lower 4 feet a variable buoyancy section. This lower section and the ballast chambers in the ends of the twin hulls are used for subsurface deployments (Fig. 4). Figure 5 shows the return-to-surface capabilities provided by the six high-pressure air cylinders mounted around the 60-inch-diameter vertical tank. Air from these bottles is used to deballast the lower section of the 60-inch-diameter vertical chamber, which raises the tower structure. A large ship-mounted compressor then deballasts the tower's pontoons.

B. Stability analysis

The flotation stability curves shown in Figures 6 and 7 were generated using DATEC's Flotation Analysis Program (FLOAT). This program solves for the theoretical equilibrium positions of floating and submerged frame composed of pipe members. The option to partially flood selected members allows simulation of a complete static upending sequence to determine possible instabilities at intermediate flooding stages. The program can also simulate concentrated gravity and buoyancy loads. The tower model was forced to rotate 45° to determine the stabilizing movements in the pitch and roll direction. The stability curves (Figs. 6 and 7) show changes in righting arm lengths with pitch and roll angles. At large pitch and roll angles there is still a positive righting arm and the tower remains in a stable, upright configuration. The dashed line on each curve is the required righting arm for the overturning moments produced by a 20-knot wind.

C. Dynamic response analysis

A dynamic response analysis was performed to determine maximum response of the tower during towing. The analysis was performed using the Ocean System Computer Analysis Routines (OSCAR) developed by Ultramarine, Inc. A frequency response analysis was made using a Pierson-Moskowitz sea-state spectrum for the sea state and tow conditions shown in Table 1.

Table 1. Pierson-Moskowitz sea-state spectrum.

Wave Height (feet)	Significant Tow Heading	Tow Speed Knots
5	Head (180°)	0
5	Bow Quartering (135°)	0
5	Beam (90°)	0
5	Head	3
5	Bow Quartering	3
5	Beam	3
1	Head	0
1	Bow Quartering	0
1	Beam	0

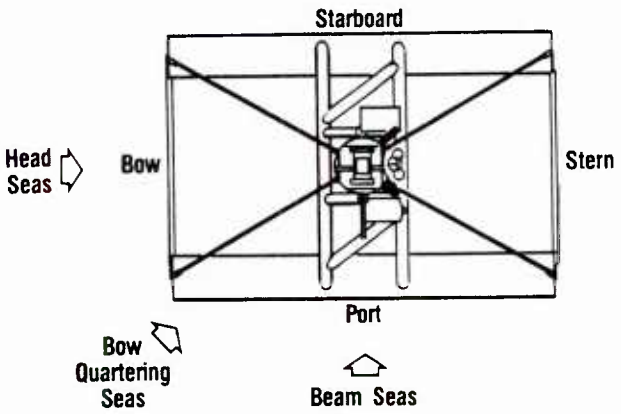

The results of these analyses are given in Tables 2, 3, and 4. The 1/10 response values are the average amplitudes (pitch angle, pitch acceleration, roll angle, roll acceleration, heave acceleration) of the highest 10% of the dynamic response values for a particular sea state. Similarly, the 1/100 values are the average of the highest 1% values. This analysis shows that for a 5-ft sea state the pitch and roll angles are within the righting arm stability envelopes given in Figures 6 and 7. The 1/100 response values were used to determine the hydrodynamic and inertial loads on the towers during tow. A structural analysis was also performed using these loads.

Table 2. Peak dynamic response (1-ft significant wave height, 1/000 responses).

		Pitch		Roll		Heave
Heading (deg)	Speed (knots)	Angle (deg)	Accel (deg/sec^2)	Angle (deg)	Accel (deg/sec^2)	Accel (ft/sec^2)
180	0	5.808	46.745	—	—	12.846
135	0	2.735	18.282	3.234	19.221	14.008
90	0	—	—	7.652	53.681	21.875

Table 3. Peak dynamic response (5-ft significant wave height, 1/10 responses).

		Pitch		Roll		Heave
Heading (deg)	Speed (knots)	Angle (deg)	Accel (deg/sec^2)	Angle (deg)	Accel (deg/sec^2)	Accel (ft/sec^2)
180	0	11.238	27.002	—	—	10.739
180	3	9.051	12.716	—	—	5.380
135	0	7.446	16.765	7.737	19.378	7.772
135	3	6.458	11.525	7.347	14.075	5.665
90	0	—	—	12.951	36.589	4.149
90	3	2.120	5.283	12.977	36.602	5.086

Table 4. Peak dynamic response (5-ft significant wave height, 1/100 responses).

		Pitch		Roll		Heave
Heading (deg)	Speed (knots)	Angle (deg)	Accel (deg/sec^2)	Angle (deg)	Accel (deg/sec^2)	Accel (ft/sec^2)
180	0	16.966	40.799	—	—	16.214
180	3	13.666	19.198	—	—	8.122
135	0	11.241	25.312	11.681	29.257	11.734
135	3	9.751	17.401	11.092	21.250	8.553
90	0	—	—	19.554	55.242	6.264
90	3	3.201	5.283	19.593	55.262	7.679

D. Tower deployment and recovery

After a suitable experimental site has been chosen, a support ship is placed in a four-point mooring (Fig. 8). The typical experimental configuration is shown in Figure 9. Each tower is towed on the surface from a staging area to the experimental site (Fig. 10). A schematic of the tower's deployment sequence is shown in Figure 11. NORDA's scientific divers open ballast valves and 4-inch-diameter seacock caps on one of the pontoons. After 4 to 5 minutes the tower is in the position shown in Figure 11A. The second hull is then flooded, and after 15 to 20 minutes the tower is in the configuration shown in Figure 11B. In this position the structure is extremely stable and behaves much as a spar buoy. The tower is now slowly towed to a marked position near the support ship. The two 4-inch-diameter seacocks are opened at the base of the 60-inch-diameter tank. A vent valve then allows the variable buoyancy tank to flood, and the tower slowly settles on the ocean bottom. This procedure is shown in Figures 12, 13, and 14. Divers then attach the source and receiving system umbilical cables from the support ship and the telemetry buoy.

Each tower is refloated by first deballasting the lower section of the 60-inch-diameter tank by using compressed air from the onboard air tanks. After deballasting, the tower is returned to the stable spar buoy configuration. Each hull is then deballasted using a high-volume air compressor located on a small support ship, and each tower is towed back to the staging port, disassembled, and returned to NORDA.

E. Transmitting system

The transmitting system utilizes a pair of broadband parametric acoustic sources to resolve the direct, bottom-reflected, and scattered signals. These sources, with their narrow-beam and low sidelobe capabilities, are ideal for shallow-water boundary scattering measurements. These sources operate over a frequency range from 15 kHz to 180 kHz with beamwidths less than 3°. Typical beam patterns at 20 kHz and 90 kHz are shown in Figure 15. Source levels at selected difference frequencies are given in Table 5. These sources were designed and calibrated by the Naval Underwater Systems Center (NUSC), New London, Connecticut.

Figure 16 is a schematic of the source transmitting and receiving (T/R) system. The T/R relay enables the scattered acoustic signals to be received conventionally on the 250-kHz transducer. The signal mixer is a double sideband suppressed carrier design. F_c is the carrier frequency, $F_{d/2}$ the difference frequency, and F_s the sampling frequency. Both sources are aimed by a triaxial positioning system. The source receiving sensitivity is shown in Figure 17.

Table 5. Parametric source.

Projectors	Difference Frequency (kHz)	Source Level (dB/μPa)
250 kHz	20	190.0
	30	197.6
	40	201.0
	50	199.4
	60	202.2
	70	201.3
	80	201.8
	90	205.5
450 kHz	90	206.9
	110	206.5
	130	208.3
	150	212.6
	180	214.2

F. Receiving systems

The receiving systems consist of the following major subsystems: a pair of multihydrophone, two-dimensional spatial arrays; two triaxial positioning systems; and a subsurface/shipboard data acquisition and computer system.

Operator control of the receiving systems is through the use of a shipboard terminal and a subsurface computer. Keyboard inputs leave via an RS 232 port and are converted to frequency shift keying (FSK) signals by the interface unit. These signals are then transmitted through the umbilical cable to the subsurface data acquisition unit. The subsurface interface unit then converts the FSK signals back to the proper direct current (dc) levels to communicate with the computer. Control links from the computer to the various units provide control signals to make the changes ordered at the shipboard terminal.

System status data from several sensors are digitized and sent to the multiplexing unit. These data are frequency modulated and transmitted up the umbilical cable to the shipboard demultiplexing unit. There, they are converted to a digital signal and passed through the FSK interface card, which adjusts the signal levels for correct inputs to the terminal. Figure 18 shows a simplified block diagram of this control system.

G. Spatial array system

The acoustic receiving systems each utilize a two-dimensional spatial array. The arrays are 19 feet long and 3 feet high, arranged in a "T" configuration. The hydrophones are EDO Model 6660 omnidirectional elements with broadband capabilities to 250 kHz. Figures 19 and 20 show the relative source-hydrophone spacings for the Panama City and Jacksonville experiments. Figure 21 shows a typical single-channel configuration. The two elliptical filters, buffer amplifier, and 40-dB gain preamplifier are an integral part of each hydrophone. The filters are required to eliminate the high-level primary frequencies transmitted by the parametric sources. The output of each hydrophone is fed to the data acquisition and computer control system housed in the electronic containment vessel located atop each tower. The output from each of the 16 hydrophones is fed through a 40-dB variable gain amplifier, band shifted to 5 kHz, low pass filtered, and FM multiplexed with 80-kHz spacing and 20-kHz modulation. Engineering data on amplifier gain states, array position, time code, and modulator frequencies are included in the multiplexed signal. The total bandwidth of the multiplexed signal is 1.8 MHz. A typical hydrophone beam pattern and frequency response curve is shown in Figure 22. The hydrophones can be positioned at any point along the array arms.

H. Data acquisition system

The subsurface data acquisition system is a computer-controlled unit that amplifies, bandshifts, and filters the 16 acoustic channels. The unit also reports time, date, status of the bandshift modulators, amplifier gains and filter settings, and monitors positioning. This information is multiplexed onto a single channel and is transmitted to the shipboard data acquisition system.

The data acquisition system consists of four main sections interconnected into a single unit. The four main electronic sections are the computer controller, the control interface, the analog receivers, and the FM multiplexer.

I. Receiver control

Any time the transmitted frequency is changed, the data acquisition system must be reconfigured to receive the new signals. This reconfiguration is done via the system control terminal. Figure 23 shows the 10 MHz phase lock signal produced by generator #1, routed through the control signal interface card where it is down converted to 5 kHz. Here it is also combined with the operator-generated signals from the terminal keyboard. This combination is routed down the umbilical cable to the subsurface data acquisition unit. These signals are conditioned by the receiver line driver and inputted to the control computer and phase lock loop (PLL) cards. The PLL card rejects the terminal signal and converts the 5 kHz to a 5.12-MHz signal retaining the phase lock with generator #1. The 5.12-MHz signal is sent to both the frequency synthesizer and the calibration synthesizer cards. This input to the frequency synthesizer, along with new commands from the computer, produces a new output signal of the proper frequency and phase to be used in the analog receiver cards. This signal is the newly assigned transmitted frequency plus 5 kHz. When this signal is modulated with the received signals in the analog receive cards, the output is a 5-kHz data signal.

The calibration synthesizer produces phase-locked signals of known parameters for injection into the analog receive cards for circuit analysis and trouble shooting. The calibration signal is routed through the control and analog receive cards. These cards also receive computer commands that cause them to address the calibrator signal input instead of the normal received signals.

J. Analog receivers

A block diagram of one of the 16 analog receiver cards is shown in Figure 24. There are four functional stages: selectors, amplifiers, filters, and modulators. In normal operation, data signals in the 10 to 200 kHz frequency range arrive at the input of the analog receiver cards and are amplified by an amount selected by the operator at the system terminal. The gains available are 2, 5, 10, 20, 50, and 100. The amplified signals are next passed through an optional prefilter that can be selected if there are problems with intermodulation products in the 25 kHz or below frequency range. The signals are then modulated with inputs from the phase-locked frequency synthesizer. The signals, which are now converted to 5-kHz signals, are inputted to the multiplexing unit. For input frequencies of 10 kHz or below, an unmodulated output can be selected.

A calibration signal generated by the calibration synthesizer can also be inputted to the analog receiver cards. It duplicates the frequency characteristics of the received signals and is used to calibrate the receiving system.

K. FM multiplexer

Figure 25 shows a basic block diagram of the multiplexing system. It consists of 16 postgain amplifiers, 20 voltage control oscillators (VCO), 1 Mux cal card, 1 mixer card, and 1 filter card containing 4 low pass filters.

Acoustic data from the 16 analog receiver cards are fed to the postgain amplifier section. The gain of these sections is set by operator via the terminal at 1, 2, 4, 8, 16, 32, 64, or 128. The signals are now passed through a 20-kHz low pass filter and inputted to the 16 VCOs. Channels 1 through 16 are used for acoustical data signals. Channel 19 is used for the computer's teletypewriter (TTY) signals. A 5-kHz phase-lock reference signal from the phase-lock loop card is filtered and impressed on channel 18. Channels 17 and 20 are blank. The 20 VCO frequencies are summed in the mixer and produce the multiplexed output signal. Table 6 lists the frequencies for each channel and the signal carried.

The Mux cal card is used when calibrating the multiplex unit. it produces output signal, which will set the VCOs at their center frequencies or to their maximum positive and negative excursions. The cal card can be controlled at the remote terminal or via switches mounted on the card itself.

L. Channel-to-channel phase characteristics

By careful selection of the electronic components it was possible to match the phase characteristics of all channels. The largest difference was between channels 7 and 8 of the forward scatter system. These measurements were taken just after the hydrophone crystal and are shown in Figure 26.

M. Array control system

The tower control system allows the operator to move the hydrophone array in roll, pitch, and azimuth.

As the diagram in Figure 27 shows, 60 Vdc from either a power supply or a battery stack is sent via the umbilical cable to the positioning system. When the operator selects the terminal key, which puts the system into the positioning mode, signals are sent via the downlink to the computer, which energizes the relays via the relay-solenoid driver card. This supplies 60 Vdc to the inverter/control unit. The computer then asks the operator to select which axis he wishes to change and how much of a change he wants. The computer then sends control signals to the reference generator card indicating which motor to activate, what direction to rotate, and for how long. The inverter section converts the 60 Vdc input to 120 Vac and the control section applies ac voltage through a control relay to the appropriate motor for as long as the input lines order.

Table 6. Channel frequency/signal.

Channel Number	Freq in kHz	Signal	Channel Number	Freq in kHz	Signal
1	80	Hydrophone	11	880	Hydrophone
2	100	Hydrophone	12	960	Hydrophone
3	240	Hydrophone	13	104	Hydrophone
4	320	Hydrophone	14	1120	Hydrophone
5	400	Hydrophone	15	1200	Hydrophone
6	480	Hydrophone	16	1280	Hydrophone
7	560	Hydrophone	17	1360	BLANK
8	640	Hydrophone	18	1440	5 kHz
9	720	Hydrophone	19	1520	TTY
10	800	Hydrophone	20	1600	BLANK

As the array is repositioned, the computer constantly reads the voltage from the sensors and updates the display for the operator. With the array repositioned, the operator normally exits the positioning mode. This causes the 60-V relays to deenergize and remove power from the inverter/control unit.

N. Array position monitoring

Figure 27 also shows the pitch, roll, and azimuthal position sensors. These receive a constant reference voltage from the reference sensor generator card. The sensors convert this constant voltage to an analog voltage that represents the position of the array. These analog voltages are sent to the computer where they, along with the reference voltage, are digitized. These digitized signals are sent through the multiplexer and the up-link system to terminal display. Roll, pitch, and azimuth are displayed in degrees (plus or minus), are displayed constantly, and are updated when the array is being repositioned.

O. Buoy electronics

Figure 28 shows the physical layout of the major components of the rf-linked buoy. Two arrays of five 12-V batteries supply a total of 60 V. Initially this power is applied only to the ±15 Vdc to dc converter, which powers only the command receiver card, the power control card, and the data amplifier card. In this idle state, minimum power is used. To activate the system, a "turn on" signal is transmitted to the buoy. This dual-tone signal frequency is modulated onto a 72-MHz carrier. This FM signal is received at the buoy via an omnidirectional antenna. The command receiver now produces an output to the power control card and sends 60 V down the umbilical cable to power up the electronics inside the instrumentation pressure vessel (IPV). The 60 V is also applied to the 30 Vdc to dc converter, which powers the buoy data transmitter. Finally, the power control card distributes ±15 V to the line-driver card, completing powering up of the buoy. Data arriving from the IPV via the umbilical cable is frequency modulated onto a 1.5 GHz carried and transmitted via an omni antenna to the ship (Fig. 29).

P. Data collection mode

Once the buoy has been fully powered up, the operator must switch to a data mode to further communicate with the system. In this mode, FSK command signals and a frequency reference signal are transmitted to the buoy and passed from the command receiver to the data amp card and into the umbilical cable. When the signals arrive at the IPV, they function in the identical way described in the hardwired system under command and control.

Q. Hardwire capabilities

The data buoy used in the forward-scatter system can be removed and the cable connecting the tower to the buoy can be brought directly to the shipboard demultiplexing unit. This procedure used is the same as that used with the backscatter tower.

This type of hardwiring is used when the forward-scatter tower is within 1500 feet of the support ship. Complete system specifications are given in Table 7.

Table 7. System specifications.

Number of acoustic channels per tower		16 ea
Bandwidth of each acoustic channel		10 kHz
Center frequency translator range	lower upper	5 kHz 200 kHz
Translating frequency sidelobes		−60 dBc
Fold-over frequency rejection @ signal frequency of 20 kHz		−30 dB
Fold-over protected bandwidth	from to	2.5 kHz 10 kHz
System noise level (re 1 V/μPa		−150 dB/V
Roll, pitch, and azimuth accuracy		1°
Hydrophone source level (re 1 V/μPa)	low gain high gain	−185 dBV −175 dBV
Variable gain	minimum maximum	0 dB 80 dB
Hydrophone spacing	minimum	2 inch

IV. Environmental measurements

A. Test site selection and characterization

Three major types of environment investigations are conducted prior to any acoustic scattering experiments.

- General large-scale areal investigations are used to identify potential acoustic measurement sites. Acoustic remote sensing methods (sidescan sonar, 3.5-kHz bottom profiles, and subbottom profiles) supported by reconnaissance bottom sampling are used in these investigations. A major emphasis is the construction of continuous sidescan sonar areal mosaics. These mosaics map and classify different bottom types, establish boundary conditions, and determine relationships between bottom types and large-scale environmental conditions.
- At selected sites within the large study areas, detailed bottom sampling provides preliminary data for classifying bottom types. These data include short-range sidescan sonar mosaics, subbottom and bathymetric profiles, sediment geological and geotechnical properties, and bottom roughness measurements. The large-scale spatial and temporal variabilities are also measured.
- Based on these large-scale areal and preliminary site studies experimental sites are selected. Extensive environmental measurements then detail the surface fine structure, geotechnical and geoacoustic properties, and spatial and temporal variabilities of the experimental sites. These data provide inputs to the acoustic scattering models and to the classification of bottom types by remote acoustic methods.

Geotechnical properties of interest include sediment grain density, porosity, grain size distribution, permeability, and shear strength. Geoacoustic properties measured are sediment compressional wave velocity and attenuation, as well as shear wave velocity and attenuation. Distribution of potential surface and volume scatterers are also determined. Both remote (grabs) and in situ (scuba-diver-collected cores, box cores, and probes) sampling techniques are used. X-radiographic cores can be collected to determine volume scatterers in soft sediments. Visual and photographic observations are also made.

Emphasis is placed on determining the spatial (vertical and horizontal) and temporal variability of all relevant geotechnical and geoacoustic properties. Fine-scale bottom roughness characteristics are determined from stereophotographic pairs and diver-collected profiles. Scales of roughness measured range from 0.5 mm to 1.0 m.

B. Sidescan sonar measurements

The sidescan sonar measurement system addresses two major requirements for high-frequency bottom-scattering experiments. The first is selection of experiment sites and the second is geologic-acoustic and bathymetric (large-scale roughness) characterizations. The sidescan sonar measurement system also details the geometry of each experimental configuration; and through the presite surveys, serves to accumulate a suite of documented "ground truth" shallow-water bottoms for constructing classifications of surface acoustic parameters (Fig. 30).

The sidescan measurement system consists of a 100-kHz sidescan sonar, a 3.5-kHz shallow subbottom profiler, a precision 24-kHz/200-kHz depth sounder, and two precision navigation systems (Fig. 31). The system is capable of rapidly acquiring a three-dimensional acoustic image of the ocean bottom. Sidescan sonar measurements provide data for high-frequency acoustics applications where surface inhomogeneities (caused by roughness and sediment properties) are more important than the deep subsurface geologic structure. A 3.5-kHz subbottom profiler is used to remotely sense bottom sediment type, and to indicate where and to what extent volume scattering may be encountered. A high-frequency narrow-beam bathymetry system complements the sidescan sonar imagery by providing accurate large-scale roughness and bottom slope data.

C. Sidescan sonar measurement system

1. Sidescan sonar towfish and data recording capabilities

The system is composed of commercially available, off-the-shelf components that provide reliability under adverse field operating conditions and an interlinking of navigational and acoustic data.

The main system component, a Klein Associates K-Maps sidescan sonar, consists of a transducer towfish, tow cable, winch, sonar transceiver with paper recorder, speed sensor, magnetic tape recorder, and signal and annotation processors. The system operates in the analog mode with the exception of the digital processors. Nominal frequency of the transducers is 100 kHz. Bandwidth is relatively large. This enhances resolution in the near- to midrange (to 100 m) over what would be expected at 100 kHz. A narrow horizontal beamwidth of 0.75° also enhances across-track resolution over that of standard 1° or 1.2° systems with some sacrifice in towing speed to maintain along-track resolution. Maximum range per transducer is 400 m (800-m swath), but in shallow water, surface noise, refraction effects and towfish altitude limit the range to 150–200 m per transducer. The towfish also carries a 100-kHz altimeter. The altimeter signal provides a strong initial bottom return, which is used by the signal processor to remove the water column. The sidescan signal can also be used for this purpose, but since this signal is tuned for uniformity across range, the initial return is often too weak to serve as an effective bottom tracker. The system has no ready provisions to tap into the received signal before it is adjusted by the time-variable gain amplifier (TVG). In shallow-water operation, the altimeter can also be used to measure water depth. Bathymetric measurements are theoretically not feasible because there is no towfish depth sensor; however, there is sufficient signal leakage that a signal with a towfish-surface-bottom-towfish path is detectable and can be used for bathymetry.

The towfish is deployed with a 200-m multiconductor Kevlar cable from a hand-operated winch fitted with slip rings. A 100-m, hand-deployable Kevlar cable serves as a backup. Depending on tow speed and water depth, either a small or a large depressor is fitted to the towfish. At speeds ranging from 1.0 to 6.5 m/sec the sidescan/altimeter towfish is stable and can be operated with or without the depressor. The winch has been adapted to be operated either by hand or through reduction gears using a detachable industrial-grade electric drill.

The towfish signals are transmitted and received by the sidescan transceiver recorder unit. Received pulses are adjusted by the TVGs and are recorded directly on a three-channel (13-cm channel width), a wet-paper recorder or on magnetic tape. Resolution and dynamic range of the wet-paper recorder are somewhat limited (Pruitt and McKinney, 1982), but the recorder can operate at high rep rates (30/sec or 25 m/channel swath width) and is relatively fume free. The tape recorder is an 8-channel Hewlett Packard model 3968A. The signals recorded by the tape deck are left and right sidescan signals, altimeter signal, timing pulse, a towing speed signal from a processor, annotation from a processor, a backup timing pulse, and voice. The recorded signals are played back through the processor for monitoring during data collection and for reprocessing the collected data in the laboratory.

Two processors are used, the Klein No. 603 and the Klein No. 606. The Klein No. 603 performs geometric corrections on the sidescan signals and creates a plane-view or map-equivalent acoustic image of the sea floor. It employs the altimeter signal to remove the water column and to correct for slant range. It also accepts a speed input to maintain the along-track scale proportional to the across-track scale.

Three sources provide speed input: from manually adjustable internal settings, from an external sensor, or computed from navigational inputs. The external sensor is an impeller mounted on a small towfish that is deployed from the vessel on its own tow cable. It accurately measures speed through the water and is responsive to small, short-term fluctuations. The electronically computed navigational speed input is subject to a significant averaging period and is thus suitable mainly for running very long straight lines. This processor also has digital speed and towfish altitude displays, and a low altitude/speed warning system.

The second processor, a Klein No. 606, provides signal expansion, delay, and annotation. The expansion capability allows enlargement of the altimeter profile while operating the sidescan at long ranges. It also enlarges items of interest while underway. For postoperational processing, it may be used to enlarge or reduce, a significant aid in sidescan sonar mosaic construction. Annotation (date, time, event number, event marking) is also supplied by the processor. It can be controlled by and messages entered from an external keyboard.

The annotation processor has been adapted to accept data streams (coordinates, latitude/longitude, speed, time) from an Internav LC303 Loran C receiver or a Motorola Miniranger C-band positioning system. The navigational input can be fed from the annotator to the speed processor and can serve as a speed input.

The Klein Associates 3.5-kHz subbottom profiler is a low-power, shallow-penetration system that is deployed as an integral attachment to the sidescan sonar system (Fig. 31). The transducer unit attaches to the sidescan towfish and is electronically connected to the tow cable with a Y-jumper cable. The jumper connects the profiler system and deactivates the towfish altimeter. (The profiler then occupies the signal path of the altimeter and also assumes its function in the sidescan system). The unit can penetrate 20 m or more in muddy sediments (1500 m/sec sound speed), but gives little or no penetration in hard-packed sands. The combined 3.5-kHz sidescan towfish is a somewhat less stable towbody and operates best at low speeds (1.5–2.0 m/sec). Its increased combined weight (over 100 kg) necessitates the use of a winch and davit during deployment and recovery.

Data recording, processing, and display of the profiler output is analogous to that of the altimeter; it senses for water column removal, and bathymetric information can be extracted as previously described for the altimeter. In playback, the expansion processor is particularly useful for examination of subbottom reflectors.

2. High-resolution bathymetry

An Odom Echotrac DF3200 depth sounder is used for precision bathymetry (Fig. 31). This is a simultaneous dual frequency unit with 24- and 208-kHz narrow-beam transducers. The larger and heavier 24-kHz transducer is suitable for deeper water or to obtain subbottom information in relatively watery sediments. The depth sounder annotates time from an internal clock and calculates and automatically displays depths at 1-sec intervals. A thermal printer is used to display these data. The unit may be interfaced with a navigation output for automated depth plotting. Presently it is operating in a standalone mode with manual synchronization of sounder and navigation clocks. The transducers are attached to temporary mounts designed to be clamped to the side of the particular boat being used.

3. Navigation systems

Two systems are available for navigation: a Loran C system based on a modified Internav LC300 receiver and a Motorola Miniranger (Falcon) IV C-band transponder system (Fig. 32). Both systems are arranged to maximize interlinkage and recording redundancy with the sidescan sonar system.

The Loran C receiver displays time differences (TDs) to 0.01 μsec, as compared to 0.1 μsec for most typical receivers. This extra precision is critical to the boat operator when running straight lines with spacings of 0.5 to 2.0 μsec (0.01 μsec corresponds to approximately 2 m). The receiver has been modified to provide multiple outputs of TDs, speed, latitude/longitude, and time. A 12-sec output is recorded on a Tektronix 4923 digital cartridge tape recorder and on a Texas Instruments Silent 700 data terminal. A 1-sec output is available to the sidescan annotation processor, where it can be displayed on demand or at 2-min and 20-sec intervals. A Racal-Decca 10350TP track plotter can be used to simultaneously provide real-time navigation plots. The operational accuracy of the Loran receiver is better than ±0.02 μsec (±4 m) when static readings are taken over some time; short-term fluctuations usually can be higher. In practice, the limit on navigation accuracy for a sidescan sonar line is the skill of the helmsman, as line deviations are generally larger than the errors of the Loran C receiver.

The Motorola Miniranger IV system produces outputs similar to the Loran C system. It provides greater positioning accuracy (±1 m) and it is preprogrammed to produce sounding plots from a direct link with the depth sounder. But the system is line-of-sight and has an approximate range of 35 km, and considerable effort is required to set up baselines, towers, and power sources.

The system consists of processor and control units, dual receiver transmitters (to reduce multipath), and four transponder units. Output (range/range or X-Y positions, time, depth) is fed to a Texas Instrument Silent 700 data terminal, a Tektronix 4923 digital cartridge tape recorder and a Houston Instrument DP-1 X-Y plotter.

The components of the sidescan sonar measurement system operate either on 110 Vac or 12-32 Vdc power. The power can be supplied by a 3-kW portable ac generator with dc power supplies provided for those components operating only on dc (Loran C receiver, depth sounder). The system can also be operated off ship's ac power through an isolation transformer or surge protectors. The dc-powered components can be wired into the ship's dc system.

4. System Operation

Through the experience of numerous field missions, a set of operating conditions has evolved that are generally applicable to shallow-water acoustic bottom characterization.

For successful operation, certain minimum vessel characteristics are required. These characteristics usually require some compromising in a typical charter boat, but any major deficiencies will adversely affect the operation. The vessel should be 12–22 m long; smaller vessels do not have sufficient space, and most larger vessels are too sluggish to maneuver precisely on the required, often small, line grids. The vessel requires a stern davit or frame to permit instrument deployment/retrieval and centerline towing, stern deck space, an air-conditioned cabin and pilot house, and dry storage space. Continuous minimum speed for towing should be 1.5–2.0 m/sec, but a high cruising speed is desirable for transit. The vessel should be equipped with an autopilot and have a responsive helm. These requirements have met with various degrees of success in the site studies conducted off Panama City and Jacksonville, Florida. The vessels used for the Panama City experiments include the R/V *Amity* of Continental Shelf Associates, an 11-m, lobster-type boat equipped with autopilot; the *Captain Gorman II*, a 15-m lobster-type boat equipped for fishing; the *Captain Gorman*, an 11-m lobster boat equipped for sports fishing; and the *PSC-12* of NCSC, a 20-m workboat-type (air-conditioned) research vessel. At Jacksonville the *NADC-23*, a 15-m harbor survey boat, and the *Lynnhaven Thunderstar*, a 19-m air-conditioned crewboat were used.

Navigation off Panama City and Jacksonville was by Loran C. Rates used were 7980-W/Y and 7990 X/Z off Panama City and 7980 Y/Z off Jacksonville. Typical long-term accuracy was about ±0.02 μsec, or roughly ±4 m. To maximize navigational accuracy, lines were run on lines of position (LOPs) maintaining one TD constant, rather than latitude/longitude. Small conversion errors in the receiver make latitude/longitude navigation by Loran C less accurate at the required large scales. Over the short distances covered, LOPs can be considered straight and

nearly parallel. Since a straight track is imperative for high-quality sidescan sonar imagery, the real limitation on navigational accuracy was the skill of the helmsman and the handling characteristics of the boat. Consistently good results were achieved with a manually assisted autopilot (only on R/V *Amity*); otherwise, acceptable straight-line steering required intense concentration by the helmsman, and a satisfactory result was not always achieved.

The operating parameters of the acoustic systems varied with range and depth. The sidescan sonar towfish is optimally flown at 1/7 of the across-track range. In practice, it was typically deployed at 8–10 m for a 50-m range, 15–18 m for a 100-m range, and 18–22 m for a 150-m range. Tow speeds were 2.0–3.3 m/sec with the altimeter fish, and 2.0–2.6 m/sec with the 3.5-kHz profiler attachment. Depending on speed and towfish configuration, tow cable payouts of 30–100 m were required to achieve the desired altitudes in the water depths under investigation (20–35 m). In shallow-water depths the sidescan system is quite sensitive to surface noise and scattering generated by waves. Generally, the presence of abundant whitecaps or seas over 1.0–1.5 m degrades the signals to an unacceptable level. The speed sensor was deployed from the side or the stern of the boat and towed 3–5 m below the surface. For bathymetric work, only the 208-kHz depth-sounder transducer was required. It was mounted 1 m below the surface and operated at speeds of 3.5–5.0 m/sec.

Sidescan signals were routed from the TVGs to the tape recorder, played back through the processor, and displayed on the wet-paper recorder as a monitor record. Tape speed was 19 m/sec (7.5 ips), which gives 1 hour of play per tape. The processors were normally set for speed, altitude, and slant range correction, and the altimeter/3.5-kHz channel displayed at 25 or 50 m full scale. Annotation generally was by 2-min event mark, with line number, date, time, Loran C TDs, latitude/longitude, and Loran C computed speed. Speed inputs to drive the sidescan sonar were from either the speed sensor or the manual inputs. Depth sounder data were recorded on paper rolls with a scan width of 10 cm and a chart speed of 5–25 m/sec. Annotation was at 12-sec intervals and corresponds to the navigation record. Navigation data (TDs, latitude/longitude, course, speed) were recorded at 12-sec intervals on digital cassette and displayed on a paper printout.

D. Sediment collection and roughness measurements

Sediment property and roughness measurements were used to classify the small-scale features of the experimental sites. Sample locations were chosen on the basis of sidescan sonar images and estimated acoustic patch size and locations. These geoacoustic and bottom roughness data also provided estimates of the spatial and temporal variabilities in each area. These data were correlated with the sidescan sonar images and provide a "ground truth" for developing bottom classification techniques. The geoacoustic and bottom roughness data were used to make scattering strength predictions prior to and during the acoustic boundary scattering experiments.

1. Sediment core collection

Sediment cores were collected by divers using cylindrical polycarbonate tubes (Fig. 33). The tubes, which measure 6.1 cm (inside diameter) by 48 cm in length, are beveled at one end to improve penetration and to minimize sediment disturbance. The tubes were carefully pushed into the bottom sediment until the divers encountered considerable resistance to further penetration. The top of the tube was sealed to retain the water overlying the sediment. Divers then carefully dug around the tube and placed a cap on the bottom end. The diver-collected cores were kept in an upright and stable condition until analyzed.

2. Sediment analysis procedure

Sediment temperature in the polycarbonate cores was equilibrated to room temperature prior to acoustic measurements. Temperature and salinity of the overlying water were measured with a YSI Model 43TD temperature probe and an AO Goldberg temperature-compensated salinity refractometer.

Values of sediment compressional wave velocity and attenuation were determined at 1-cm intervals in the core samples with an Underwater System, Inc. (Model USI-103) transducer-receiver head. A Tektronix PG 501 pulse generator and FG 504 function generator, Krohn-Hitz 3100R band pass filter, and a Hewlett-Packard 1743A dual-time interval oscilloscope were substituted for the electronics unit and oscilloscope usually employed with the USI-103 velocimeter. These substitutions increased resolution of compressional wave velocity measurements and provided accurate measurement of received voltages required for attenuation measurements (Fig. 34).

The measurements were taken with a 400-kHz, 25 μsec long continuous wave (CW) pulse. The received signal was high and low pass filtered (1–1000 kHz) prior to making time delay and received voltage measurements. Time delay measurements and received voltage measurements were made utilizing the maximum peak height of the fourth sine wave peak.

3. Roughness measurements

Roughness of the sediment-water interface was measured using two diver-operated systems. A manual roughness profiling apparatus was used to trace a 1.8-m-long section of the sediment water interface on a sheet of Mylar (Figs. 33 and 35). The measuring apparatus consists of a 1.8 m by 0.4 m sheet of 0.6-cm-thick Plexiglas with an attached level. The apparatus can be pushed into the sediment or held a few centimeters above by its support legs. After leveling, the interface is traced on gridded Mylar sheets. The accuracy of the system is dependent on the bottom type,

currents, visibility, and skill of the diver. Operational tests have shown accuracies of better than 0.5 cm in both the horizontal and vertical axis.

Roughness measurements were also made with a Photosea Model 2000 diver-operated 35-mm stereo camera. The camera uses two Nikon 28-mm, water-corrected lenses separated by 6.1 cm. A Photosea Model 1000 strobe delivering 100 W/sec was used as the light source. The stereophotogrammetric roughness profile apparatus is mounted in a rigid PVC frame to maintain a constant orientation and distance above the bottom (Figs. 33 and 36). At the 91-cm height from the bottom, the effective overlap area is 54 by 74 cm.

Stereophotographs for both experiments were made on 10-m strips of Kodak ISO 64 Ektachrome film, usually with a focal length setting of 68 cm and an f-stop of 8. The camera is equipped with enough film for 100 stereophotographic pairs. A glass "Reseau" plate imposed a precise arrangement of fiducial marks for subsequent photogrammetrical analysis on each pair of stereophotographs. A 50-foot (15.2 m) tape measure is staked down on the bottom to be photographed (Fig. 33). The orientations of the tape are parallel and perpendicular to the azimuthal angle of the transmitted acoustic signals. A series of stereophotographs are then taken along the tape such that each stereo pair is contiguous or slightly overlaps with adjacent stereo pairs. In this way, adjacent stereo pairs may be juxtaposed in analysis to create a pathlength greater than that existing in a single stereo pair (54 cm).

4. Underwater video camera

Visual observations of the area around each experimental site were made with a remote Sea Bee CM-50 underwater color video camera. Underwater lighting was provided by a MK13AS 500 W/sec quartz iodide lamp assembly. The video camera and lamp are attached to a Plexiglas vane, as in Figures 33 and 37. The camera is oriented at a 30° angle to the horizontal, and the lamp is adjusted to illuminate the oncoming field of view as the vessel drifts and the vane orients itself into the direction of movement. Use of the remote video camera at the experiment sites provides observation of a much greater area than is afforded by divers' observations. Real-time observation or subsequent analysis of videotaped images confirms the homogeneity of the bottom and provides data on any biological activity that might affect the bottom at each of the experimental sites.

V. Experimental measurements

Two ocean bottom scattering experiments have been conducted. The first site was located 19 miles south of Panama City, Florida, in a water depth of 100 feet (Fig. 38). This area was chosen for its simple and uniform bottom characteristics. The bottom was mainly fine sand with little shell content and a very small surface roughness.

The second experiment site was off Jacksonville, Florida, in a water depth of 90 feet (Fig. 39). The bottom in this area was mainly medium to coarse sand but was characterized by a coarse (gravel size) shell hash distributed in alternating bands of abundant and scarce concentrations.

Figures 40 and 41 show sidescan mosaics of each site and its relationship to the surrounding region. Preliminary high-resolution bathymetry of each area is shown in Figures 42 and 43.

A third experiment is planned for August 1987 in an area 25 miles south of Panama City, Florida (Fig. 38). This site is composed of medium to fine sand that is loosely packed, well sorted, and relatively free of shell fragments, but the surface roughness is determined mainly by sand ripples.

A. Acoustic measurements

Acoustic bottom scattering measurements have been made at two experimental sites. Measurements of both bottom forward and bottom backscattering have been made as a function of frequency, grazing angles, pulse length, azimuthal angles, and environmental parameters. Table 8 outlines the available environmentally supported acoustic data taken from both sites.

Table 8. Acoustic bottom scattering measurements.

Measurement	Panama City	Jacksonville
Bottom backscattering	29-180 kHz parametric	20-180 kHz parametric
	20 and 90 kHz conventional	20 and 90 kHz conventional
	200 μsec to 10 msec	200 μsec to 20 msec
	19-21 kHz linear sweep	3° to 30° grazing angle
	1-30° grazing angles	0° and 90° azimuthal angles
	0° and 90° azimuthal angles	
Bottom forwardscattering	20, 60, 90 kHz	
	200 μsec to 10 msec	
	Direct, 11° grazing angle	

B. Sidescan sonar measurements

Sidescan sonar and high-resolution bathymetric measurements have been made at the Panama City and the Jacksonville sites. These data include presite bathymetry and sonar images. Data were also taken to characterize the experimental area and final experimental configurations. The data include multiple sidescan sonar mosaics at 150-m, 100-m, and 50-m ranges; 3.5-kHz subbottom profiles; and closely spaced bathymetric tracks. At the Jacksonville site, sediment acoustic data were collected with an ELAC sediment classifier.

C. Sediment and roughness measurements

Sediment sampling and roughness measurement locations were chosen on the basis of sidescan sonar imagery and are representative of the experimental areas. Cores, roughness measurements, and video camera stations were taken along the acoustic footprints and at other selected positions. Table 9 outlines the sampling activities and locations for both the Panama City and Jacksonville experiments.

D. Oceanographic measurements

Temperature and sound speed profiles were recorded every 4 hours using standard CTD equipment. These data will be used to determine acoustic incident angles, insonified areas, and propagation loss values.

VI. Data analysis

A. Sidescan sonar and bathymetry analysis

The general areas of data reduction are navigation track editing and plotting, constructing bathymetric maps, reprocessing sidescan imagery and subbottom profiles, and constructing sidescan mosaics.

Navigation data is processed to obtain edited and corrected navigation plots of track lines on a mercator projection. The navigation plots are used to construct bathymetric maps and with sidescan data for image processing and assembling mosaics. Navigation processing is performed on a VAX 11-750 through a series of steps that allows the shallow-water data to be run on NORDA's existing plotting programs. Originally designed for small-scale, large-area ocean surveys, these programs can accurately plot at scales of 300 inches/degree (7.5 m/degree) or better. Initially, navigation data is downloaded from digital cassette to disk on the VAX via a modem. The downloaded data is edited and line feeds are removed from the data. Loran C time differences are then converted to high-precision geographic positions (latitude/longitude). At this stage, the desired track lines are extracted from the navigation file by time brackets. The positions on the extracted track lines are converted to a file that is compatible with the plotting program. These files, coming from various cassettes, are combined as necessary, read out as a listing, and plotted on a CalComp plotter at an appropriate scale.

Sounding data are processed to produce computer-generated sounding sheets from which bathymetric maps are constructed. Sounding profiles from the chart recorder are digitized on a digitizing table and downloaded to the VAX. Files are created for each trackline and interpolated times are assigned to the digital depths. The digitized depth files are then merged with the navigation files. The merged files are plotted as a sounding sheet. As with navigation lines, sounding lines for a given area must be combined before they are plotted. If necessary, a depth adjustment is applied and a tide correction made to the depth files before they are plotted. A polynominal function is fitted to the tidal curve for the desired time and location and is then applied to the sounding lines. For the offshore locations at Panama City and Jacksonville, tides had to be extrapolated from nearby coastal reference points. Contouring the sounding sheets is best accomplished manually if the most accurate bathymetry is desired. The investigator's knowledge of the bottom from the sounding profiles, sidescan data, and other sources, plus his recognition of potential biases caused by line and sounding spacings, are more likely to result in a truer representation of the bottom than strictly automated contouring routines. A display program is used to produce generalized contour maps and to provide three-dimensional displays of the bottom. This program grids the data and is more successful for smooth, undulating bottoms represented by evenly spaced data points, but causes persistent biases in irregular and patterned bottoms, such as a sand ridge topography.

Sidescan imagery and 3.5-kHz subbottom profiles can be reprocessed on playback to improve the quality of the display. Enlargement is through the expansion/delay processor. The tape playback speed is reduced for additional enlargement and is useful for subbottom profiles. Some contrast enhancement can be achieved through a combination of adjustments to the tape output levels and the print and threshold settings of the chart recorder. The print and threshold levels can also be used as filters; e.g., with a high threshold setting, high-intensity targets can be displayed without bottom backscatter. Speed adjustments on the correction processor are used to make scale adjustments. Geometric correction processing can be bypassed for improved near-field imaging. In general, the processing capabilities of the sidescan sonar system are limited, and external digital image processing is needed to make the best use of all the information contained in the signals.

Sidescan mosaic construction is conducted manually and consists of reduction of sidescan imagery and matching it to tracklines. Reduction is accomplished initially with the expansion processor in a reduction mode with the appropriate speed adjustments. After the overlapping trackline strips are assembled and mounted on a backing, the complete mosaic is photographed. Matching the image strips to the tracklines takes into account the towfish layback from the navigation antenna. This match requires a compromise between speed adjustment, trackline straightness, and quality of fit to produce a mosaic that is least

Table 9. Summary of sampling activities for experiments at Panama City (dives 58–76) and Jacksonville (dives 101–115). (BST = backscatter tower; FST = forwardscatter tower).

Dive No.	Date	Depth (m)	Location	Samples Collected
58	23 August 1984	34	29°51.4′N; 85°47.0′W	2 cores
59	24 August 1984	34	29°51.4′N; 85°47.0′W	2 cores
68	14 September 1984	34	29°51.2′N; 85°47.0′W (BST)	2 cores
69	14 September 1984	34	near BST	2 cores, stereophotos
70	15 September 1984	34	near BST	manual profiles
—	15 September 1984	34	between BST and FST	video camera
72	15 September 1984	34	near BST	biological samples
73	16 September 1984	34	20 m from BST @ 190°	2 cores
74	16 September 1984	34	20 m from BST @ 210°	manual profiles
75	17 September 1984	34	45 m from BST @ 270°	2 cores, stereophoto
76	18 September 1984	34	80 m from BST @ 280°	3 cores
—	31 July 1985	27	30°36.3′N; 80°53.6′W	video camera
101	15 August 1985	27	30°36.1′N; 80°53.5′W (BST)	2 cores
102	15 August 1985	27	between BST and FST	manual profile
103	15 August 1985	27	between BST and FST	stereophotos
104	16 August 1985	27	between BST and FST	2 cores
105	16 August 1985	27	between BST and FST	2 cores
107	16 August 1985	27	25 m from BST @ 150°	1 core
108	17 August 1985	27	55 m from BST @ 250°	2 cores
109	17 August 1985	27	25 m from BST @ 250°	2 cores
110	17 August 1985	27	between BST and FST	surface samples
111	17 August 1985	27	25 m from BST @ 150°	stereophotos
112	18 August 1985	27	near FST	2 cores
113	18 August 1985	27	near FST	stereophotos
114	19 August 1985	27	near BST	oblique photos
115	19 August 1985	27	near BST	shell band measurements

distorted and capable of being interpreted. It must be kept in mind by the viewer that the straight tracklines so evident on most mosaics are artifacts and imply a greater image veracity with respect to geographic coordinates than actually exists.

B. Sediment Analysis

Sediment compressional wave velocity is determined by comparison of similar time delay measurements made on the overlying salt water and sediments using the following equation:

$$V_{(s)} = \frac{V_{(w)}}{1 - \frac{\Delta t\, V_{(w)}}{d}},$$

where $V_{(s)}$ is the sound velocity through sediment (m/sec); $V_{(w)}$ is the sound velocity through distilled water (m/sec); Δt is the measured time arrival through sediment (sec); and d is the inside diameter of the core (m). All sound velocities are calculated at the temperature, salinity, and pressure (23°C, 35 ppt, 1 atm) suggested by Hamilton (1971) and at the approximate in situ conditions at time of collection (24°C, 36 ppt, 34 m for Panama City; 27°C, 35 ppt, 27 m for Jacksonville). A normalized sound velocity expressed as the velocity ratio (V_{ratio}) represents the ratio of sound velocity in sediment to sound velocity in the overlying water. Figure 44 shows a typical vertical distribution of sediment velocity ratio at the experiment site off Panama City.

Attenuation measurements are calculated as 20 log of the ratio of the received voltage through distilled water versus received voltage through sediment. Attenuation measurements are extrapolated to a 1-m path length and are reported as dB/m. Attenuation is also expressed as a sediment specific constant (k):

$$\alpha = kf^n,$$

where α is the attenuation of compression waves in sediment (dB/m), f is the transmitted signal frequency (kHz),

and n is a measure of frequency dependence. If n is assumed to be 1 (Hamilton, 1972), then the sediment specific constant (k) can be used to compare sediment attenuation to other sediment physical properties, such as porosity and mean grain size, without regard to the frequency at which the measurements were made. Figure 45 shows the relationship between attenuation (k) and depth within the sediment at the experimental site off Panama City.

After acoustic measurements are made, sediments are extruded and sectioned at 2-cm intervals for grain size, porosity, and bulk grain density analysis. Sediment grain-size distributions are determined for all sediment samples by dry sieving the samples on a set of sieves of ¼ ϕ increments on a CE Tyler sieve shaker for gravel and sand-sized particles. The pipette method is used to determine the percent of silt and clay in each sample. Mean ϕ, standard deviation, skewness, kurtosis, and normalized kurtosis are calculated according to the graphic formulae of Folk and Ward (1957). An example of grain-size data plotted as weight-percent histograms and a cumulative weight curve is displayed in Figure 46. The distribution of mean grain size with depth in the sediment for the Panama City experiment site is shown in Figure 47. Porosity is determined as weight loss of sediment dried at 105°C for 24 hours. Values of porosity are not corrected for pore water salinity. Salt-free porosity values can be calculated by multiplying reported values by 1.012. Figure 48 shows the vertical distribution of sediment porosity at the Panama City experiment site. Sediment grain density is measured on dry samples with a Beckman Model 930 Air Comparison Pycnometer and a Sartorius MP 1212 balance (precision ±1 mg). A preliminary vertical distribution of average sediment grain density at the Jacksonville experiment site is shown in Figure 49.

Seawater density, $\varrho_{(w)}$, is calculated from the Knudsen hydrographic tables given salinity and temperature. Values are accurate to 1 x 10^{-5} g/cm^3. Seawater impedance $I_{(w)}$ is calculated as the product of seawater density $\varrho_{(w)}$ and in situ compressional wave velocity $V_{(w)}$.

$$I_{(w)} = \varrho_{(w)} \times V_{(w)}$$

Sediment compressional wave velocity $V_{(s)}$ at in situ conditions is calculated as the product of the compressional wave velocity ratio $V_{(ratio)}$ and the in situ seawater velocity $V_{(w)}$ (Hamilton, 1970).

$$V_{(s)} = V_{(ratio)} \times V_{(w)}$$

Sediment density $\varrho_{(s)}$ is calculated from the proportional porosity (n) and seawater density $\varrho_{(w)}$ using a sediment grain density of 2.65 g/cm^3 (quartz sand) or an average grain density $\varrho_{(G)}$, as determined with the pycnometer (for shell-rich sediments).

$$\varrho_{(s)} = n\varrho_{(w)} + (1-n)2.65$$

or

$$= n\varrho_{(w)} + (1-n)\varrho_G.$$

The Rayleigh reflection coefficient (R) for compressional waves at normal incidence to the sediment-water interface is calculated as the impedance mismatch between water $I_{(w)}$ and sediment $I_{(s)}$.

$$R = \frac{I_{(s)} - I_{(w)}}{I_{(s)} + I_{(w)}}$$

Bottom loss (BL) is calculated in decibels.

$$BL = -20 \log R$$

The critical angle $\theta_{(c)}$ is calculated as a function of the velocity ratio $V_{(ratio)}$.

$$\theta_{ac} = \cos^{-1} \frac{1}{V_{ratio}}$$

Table 10 displays measured and calculated sediment geoacoustic properties for the Panama City and Jacksonville experiment sites. Values of sediment compressional wave attenuation were measured at 400 kHz at Panama City and 120 kHz at Jacksonville.

C. Bottom Roughness Analysis

Preliminary estimates of bottom roughness are calculated from manual roughness profiles. Bottom traces are digitized at 0.5-cm intervals with 256 points per trace. A representative profile is presented in Figure 50. RMS roughness is calculated as the standard deviation of the mean height for the 256 points. The value of manual roughness profiles is in the acquisition of a rapid estimate of RMS roughness in the field. RMS roughness estimates, as well as sediment velocity and density ratios, are used to make predictions of acoustic bottom backscattering as actual acoustic data is collected.

Analysis of stereophotographs for measurement of bottom roughness is more precise and labor intensive than for manual profiles. The fiducial marks imposed on the stereophotographs by the Reseau plate are used as reference points for visual parallax measurements with the Seagle 90 Subsea photogrammetric stereocomparator (Fig. 51). A Zenith 248 microcomputer (through an RS-232 serial interface) runs the photogrammetry software, which corrects for light distortion caused by refraction in salt water and lens aberration. The stereocomparator is capable of measuring x, y, and z coordinates within the stereophotograph overlap with an image resolution of 0.005 mm in the x and y axes and 0.001 mm in the z, or height, axis.

Relative sediment height is determined from a series of stereophotographs in which equally spaced points along

Table 10. Preliminary measured and calculated sediment geoacoustic properties for experimental sites at Panama City and Jacksonville.

Measured Properties	Panama City	Jacksonville
Depth (m)	34	27
Temperature (°C)	24	27
Salinity (ppt)	36	35
Porosity (%)	39.0	39.3
Mean grain size (ϕ)	2.59	0.67
Velocity ratio *	1.133	1.107
Attenuation (k)*	0.59	1.47
Calculated Properties		
V_p^* (m/sec)	1.737	1.711
Density (g/cm^3)	2.016	2.035
Impedance (g/cm^2 sec x 10^3	3.50	3.45
Rayleigh Reflection Coeff.	0.381	0.373
Bottom loss (dB)	8.4	8.6
Critical angle (deg.)	28.0	24.7

* @400 kHz for Panama City data; 120 kHz for Jacksonville data

a pathlength not less than 100 cm are used. RMS roughness is calculated as previously described. The power spectral density function is estimated for each pathlength.

D. Acoustic data analysis

The multiplexed signal from each array is recorded on a Honeywell Model 101 analog tape deck. Clock signals, gate pulses, transmittal wave forms, the scattered signal received on the 200-kHz source, and sampling signals are recorded on the remaining channels. The multiplexed signal is played back through a demodulating system. Each of the hydrophones and outputs is amplified, filtered, and fed to a PDP 11/34 computer and array processing system. The gate and sampling signals are shaped and used as the A/D trigger and clock pulses. The signals are digitized by a Computer Design and Application multichannel array processor. This is a 12-bit system and therefore has adequate dynamic range. This playback system is shown in Figure 52.

The narrowband modulator outputs have been modulated down to 5 kHz irrespective of the transmitting frequency. The digitizing process is an approximation of quadrature sampling and is valid when the signal bandwidth is small compared to the carrier frequency. Because the sampling process takes place at 20 kHz (four times the carrier frequency), two samples are taken 90° out of phase. These samples, x and y, then form a quadrature pair and are used to calculate an envelope value at the average of the two sampling times.

$$(e_{ij})^2 = (x_{ij}^2(n) + y_{ij}^2(n))$$

where $x_{ij}(n)$ and $y_{ij}(n)$ are the nth quadrature pair of ping i and hydrophone j. $e_{ij}(n)$ is the envelope value for each nth quadrature pair of ping i and hydrophone j.

The envelopes for each pulse and hydrophone are averaged over the number of pings

$$E_{ij}(n) = \frac{1}{N} \sum_{i}^{N} e_{ij}^2(n) \qquad j = 1, 2, 3 \ldots ,$$

where N is the number of pings.

Scattering strengths are estimated from the acoustic measurements, where scattering strengths per unit area is defined as

$$SS = 10 \log \frac{I_s}{I_i}$$

where I_i is the incident intensity, I_s is the scattered intensity. Because measurements of I_i and I_s are not practical, scattering strengths are estimated from the sonar equation and can be written as

$$SS = RL - SL + 2TL - 10 \text{ Log (area)} - 10 \text{ Log } (D_p(\theta_1)) - 10 \text{ Log } (D_h(\theta_2))$$

where

$D_p(\theta_1)$ = *projector directivity function as a function of the angular separation between the maximum response axis (MRA) and the 3 dB downpoints*

$D_h(\theta_2)$ = *hydrophone directivity function as a function of the angular separation between the MRA and the 3 dB downpoints*

and where SS = scattering strength in dB/m^2,
RL = received level in dB,
SL = source level in dB re 1 μPa at 1 m,
TL = transmission loss in dB,
A = effective bottom area in m^2.

Correlation functions are computed as functions of signal power. The normalized power cross-correlation estimates are then defined as

$$C_p(\tau) = \frac{\sum_{i=m}^{M+N} x^2(i)\, y^2(i+\tau)}{\left(\sum_{i=m}^{M+N} x^4(i) \sum_{i=m}^{M+N} y^4(i) \right)^{1/2}} ,$$

where $x^2(i)$ and $y^2(i)$ are the series power samples. The results of the cross-correlation analysis will then be compared to hydrophone spacings, transmission frequency, and the different bottom parameters. Normalized scattering strengths (SS) will be used to determine the frequency dependence and distribution functions:

$$SS_0 = SS - 20 \log \sin \theta_G ,$$

where θ_G is the grazing angle.

Because of the length of the receiving arrays, out-of-plane scattering will also be common to the various acoustic and environmental conditions.

Coherence estimates will provide a measure of the causality on a per frequency basis between the transmitted and received signal at each hydrophone. The coherence function is defined by

$$\gamma^2 = \frac{\overline{|G_{yx}|}^2}{\overline{G_{xx}}\ \overline{G_{yy}}}$$

where G_{yx}, G_{xx}, and G_{yy} are estimates of the cross-power spectrum, input power spectrum, and output power spectrum.

One of the goals of the program is to verify or to develop acoustic scattering models that are needed by the high-frequency community for performance predictions and design tradeoff decisions.

Resonance, facet, and point scatter models will be considered. All these models have as inputs such bottom parameters as roughness and geoacoustic properties. Because this program's experiments have been designed to highlight some of the important scattering mechanisms, the data will serve as an excellent test of these models and their range of applicability.

VII. References

Briggs, K. B., P. Fleischer, R. I. Ray, W. B. Sawyer, D. K. Young, M. D. Richardson, and S. Stanic (1986). *Environmental Support for a High Frequency Acoustic Bottom Backscatter Experiment off Charleston, South Carolina, 17-28 June 1983*. Naval Ocean Research and Development Activity, NSTL, Mississippi, NORDA Report 130, 86 pp.

Boehme, H., N. P. Chotiros, L. O. Rolleigh, S. P. Pitt, A. L. Garcia, T. G. Goldsberry, and R. A. Lamb (1985a). Acoustic Backscattering at Low Grazing Angles from the Ocean Bottom. Part I. Bottom Backscattering Strength. *J. Acoustic Soc. Am.* 77, 962-974.

Boehme, H., N. P. Chotiros and M. P. Churay (1985b). Bottom Acoustic Backscattering at Low Grazing Angles in Shallow Water. Part I. Bottom Backscattering Strength. *Proc., Int. Acoust.* 7, 19-26.

Folk, R. L. and W. C. Ward (1957). Brazos River Bar, A Study in the Significance of Grain Size Parameters. *J. Sediment. Petrol.* 27, 3-26.

Hamilton, E. L. (1970). Reflection Coefficients and Bottom Losses at Normal Incidence Computed from Pacific Sediment Properties. *Geophys.* 35, 995-1004.

Hamilton, E. L. (1972). Compressional Wave Attenuation in Marine Sediments. *Geophys.* 37, 620-645.

Jackson, D. R., D. P. Winebrenner, and A. Ishimaru (1986). Application of the Composite Roughness Model to High Frequency Bottom Backscattering. *J. Acoust. Soc. Amer.* 79, 1410-1422.

McKinney, C. M. and C. D. Anderson (1969). Measurements of Backscattering of Sound From the Ocean Bottom. *J. Acoustic Soc. Am.* 36, 158-163.

Pruitt, J. G. and C. M. McKinney (1982). *A Study to Determine the Feasibility of Using the Klein 500 Sonar to Make Quantitative Bottom Backscattering Measurements*. Applied Research Laboratories, University of Texas, Austin, Technical Report ARL-TR-82-33, 49 p.

Richardson, M. D., K. B. Briggs, R. I. Ray, and W. H. Jahn (1986). *Environmental Support for High Frequency Acoustic Experiments Conducted at the Quinault Range, April-May 1983*. Naval Ocean Research and Development Activity, NSTL, Mississippi, Report 132, 76 pp.

Urick, R. J. (1975). *Principles of Underwater Sound*. New York, McGraw-Hill.

Wong, H. K., and W. D. Chesterman (1968). Bottom Backscattering Near Grazing Incidence in Shallow Water. *J. Acoust. Soc. Am.* 44, 1713-1718.

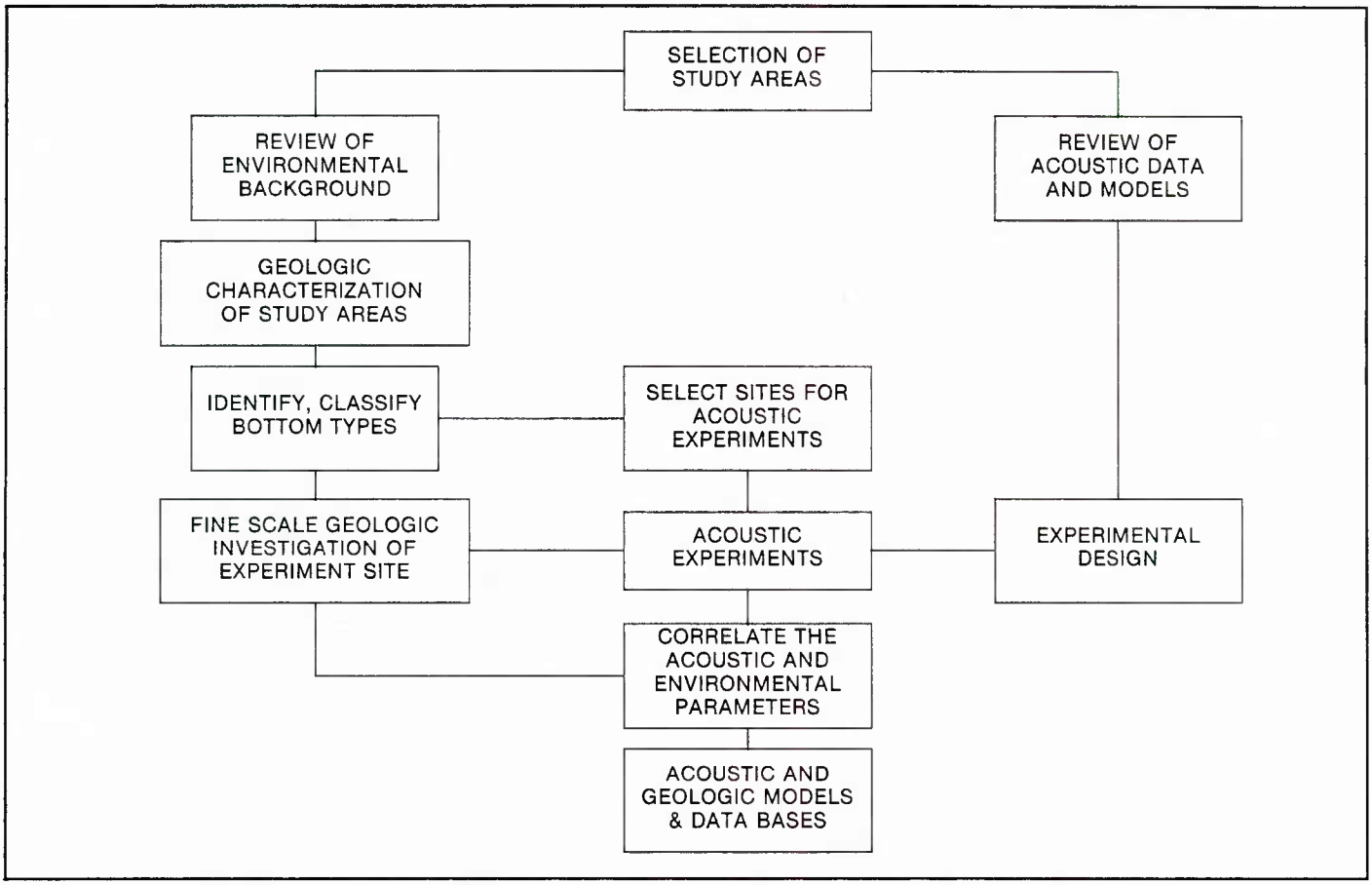

Figure 1. Relationships between the acoustic and geological experiments.

Figure 2. NORDA's shallow-water acoustic measurement systems.

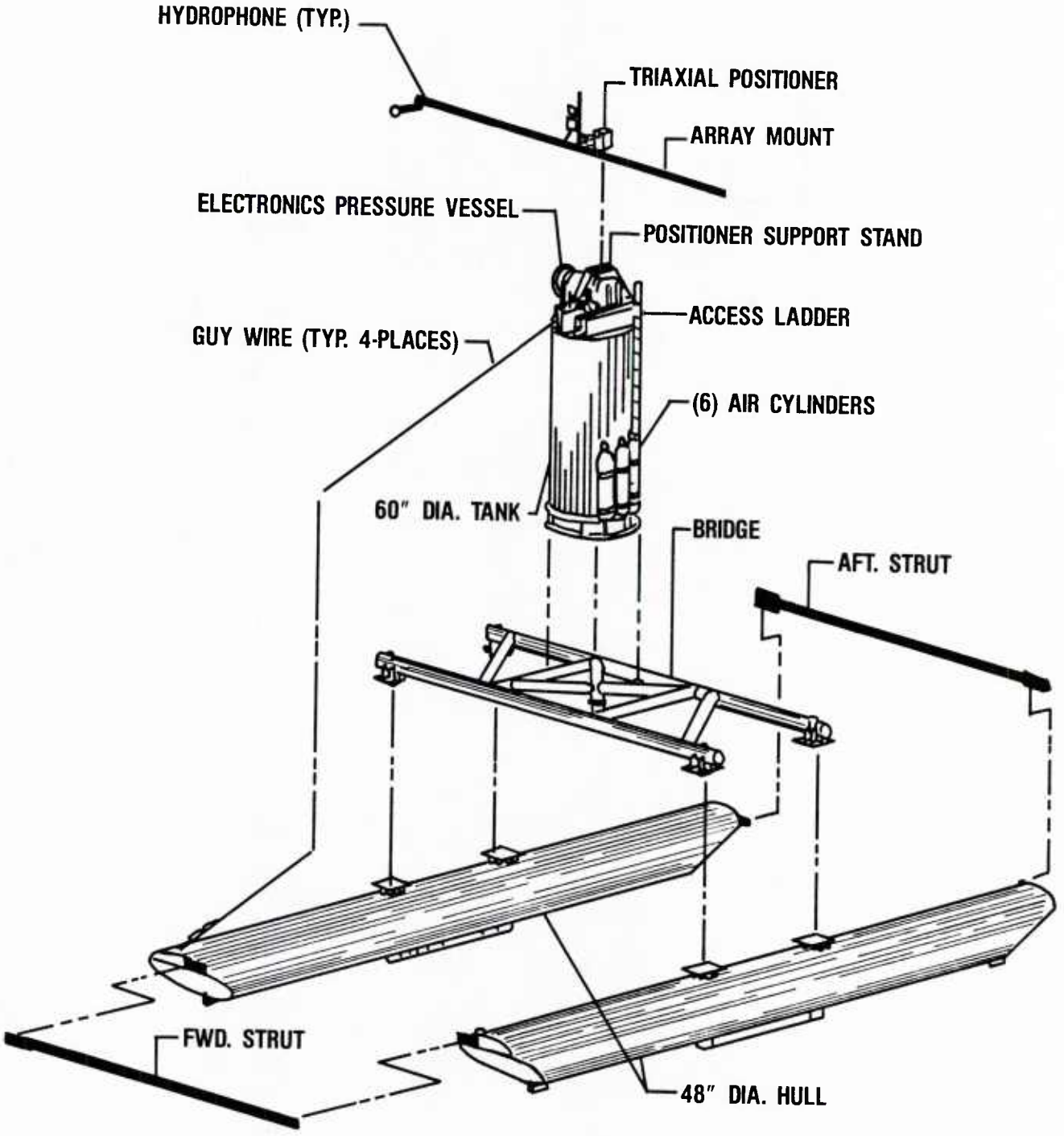

Figure 3. Major tower subassemblies.

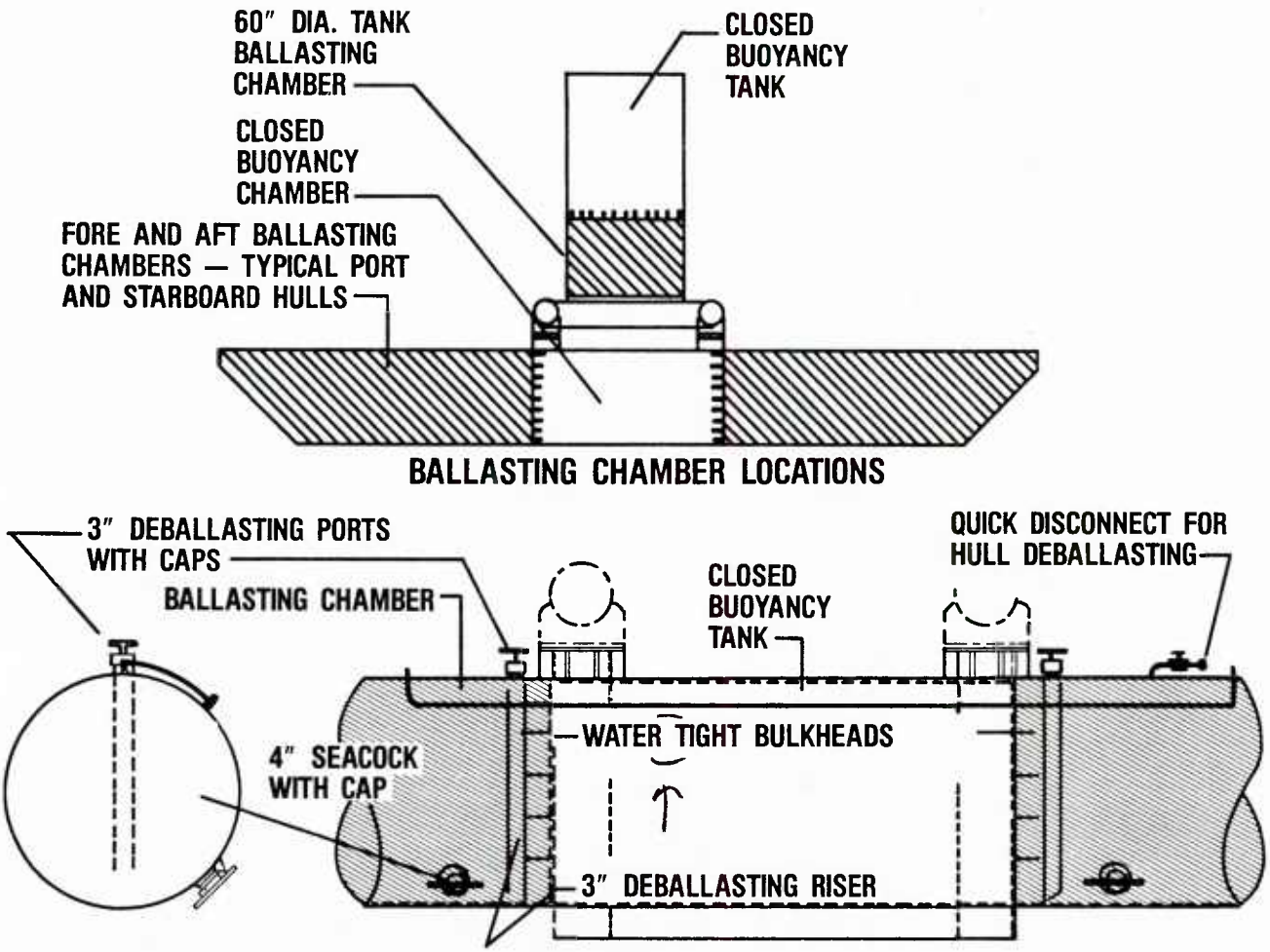

Figure 4. Tower ballast/deballast systems.

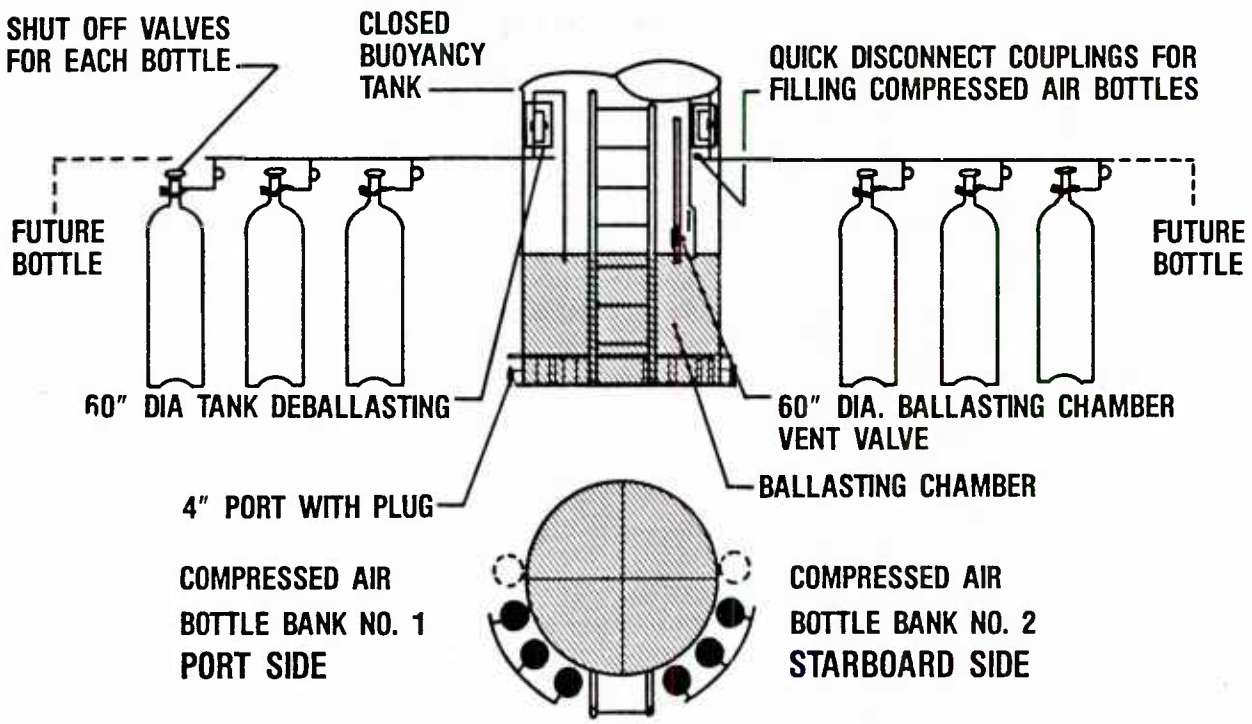

Figure 5. The 60-inch-diameter tank ballast/deballast system.

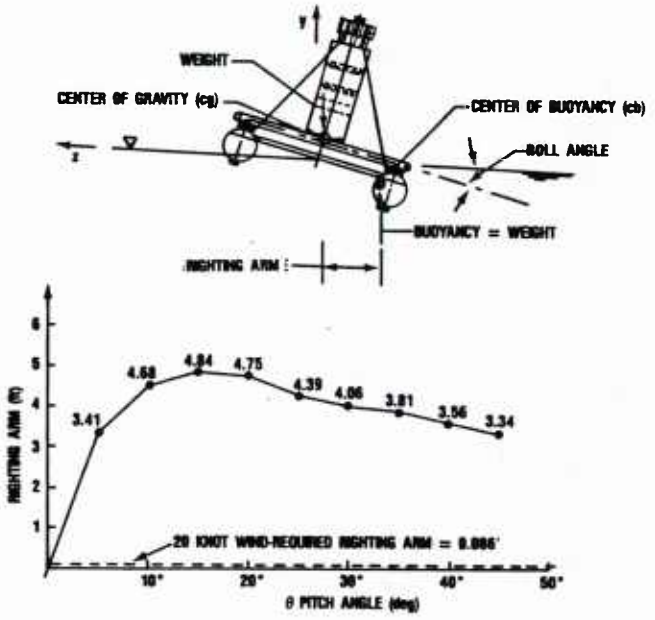

Figure 6. Stability curve.

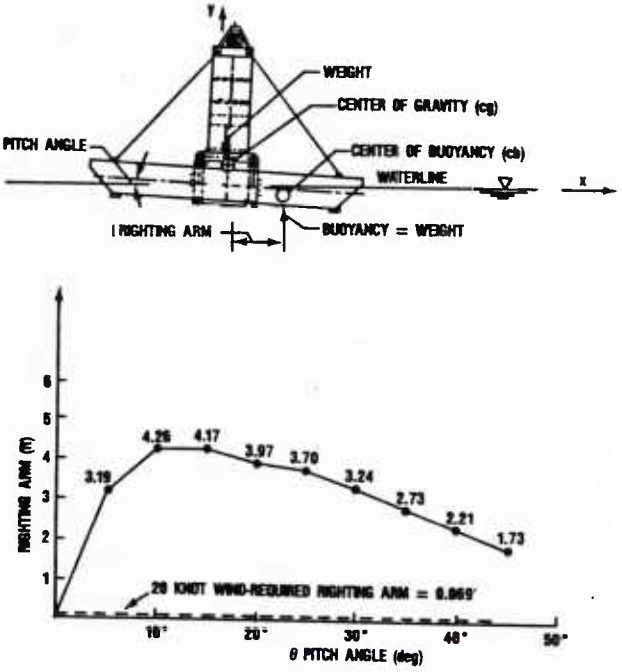

Figure 7. Stability curve.

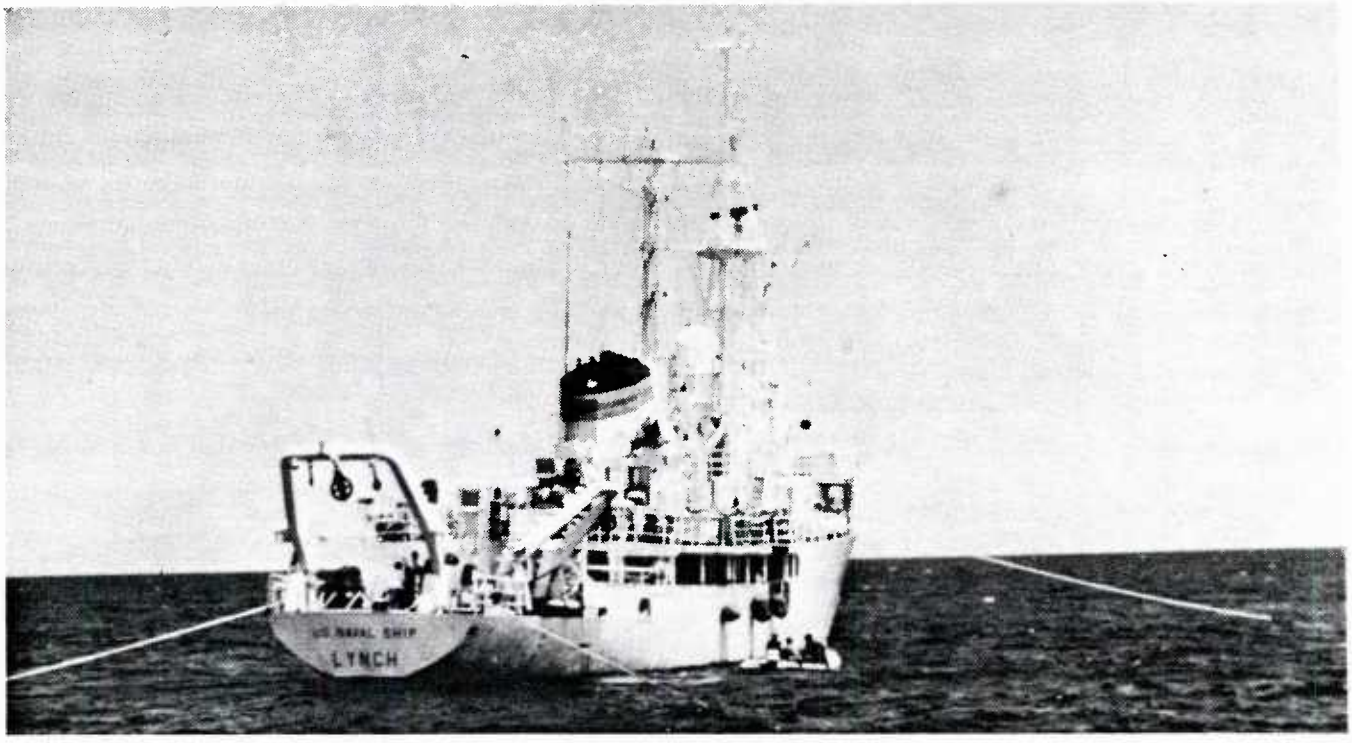

Figure 8. U.S.N.S. Lynch *in a four-point mooring.*

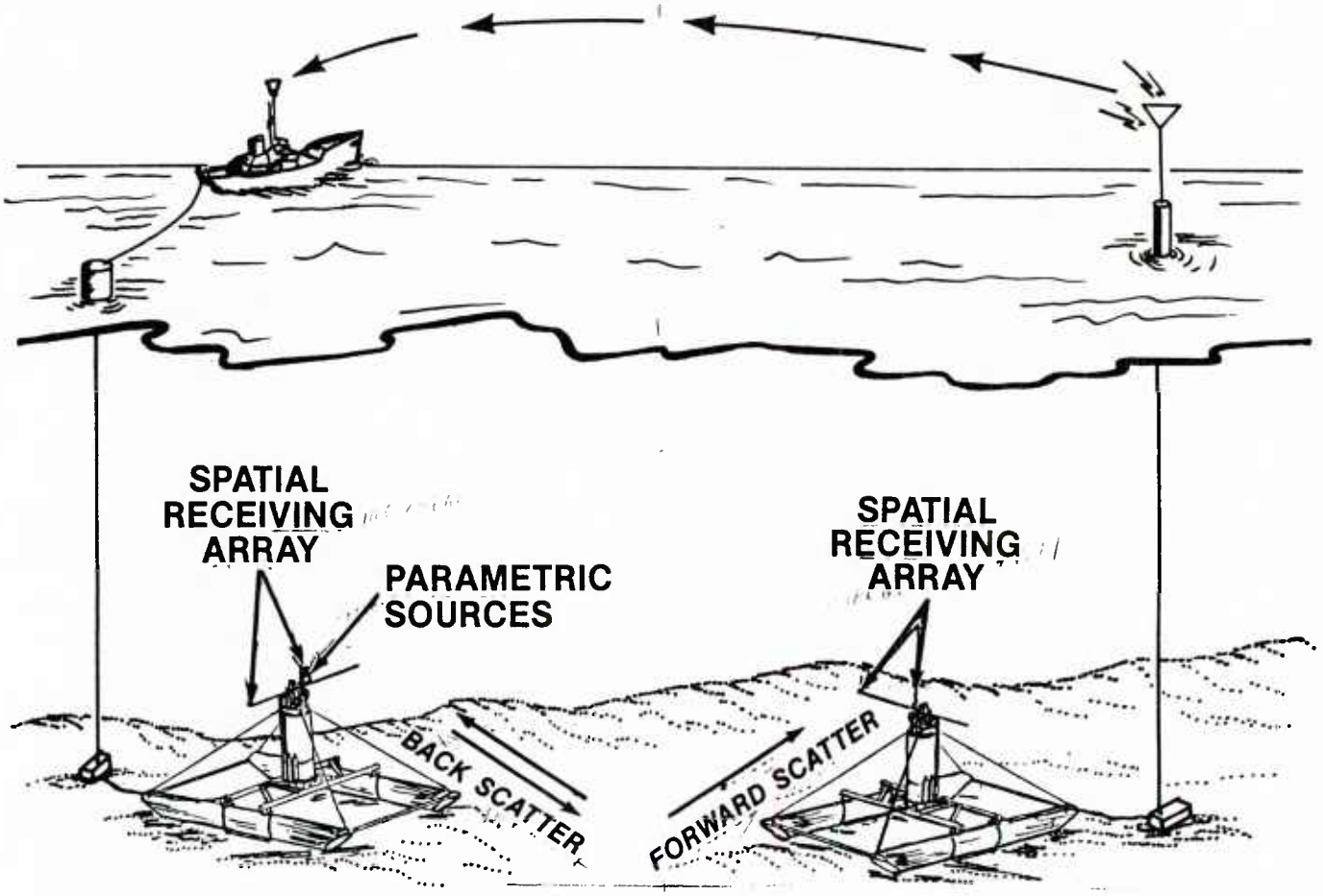

Figure 9. Experimental configuration.

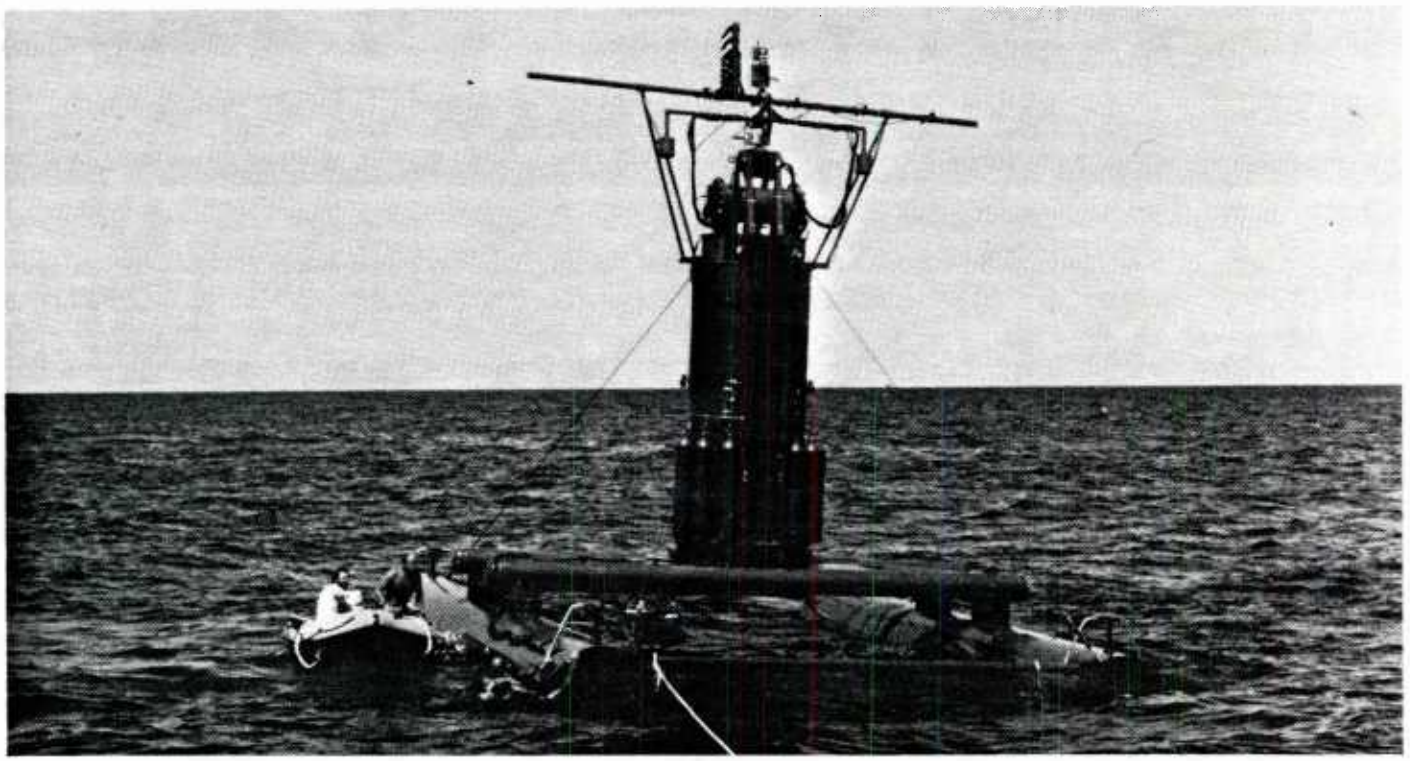

Figure 10. Tower being prepared for deployment.

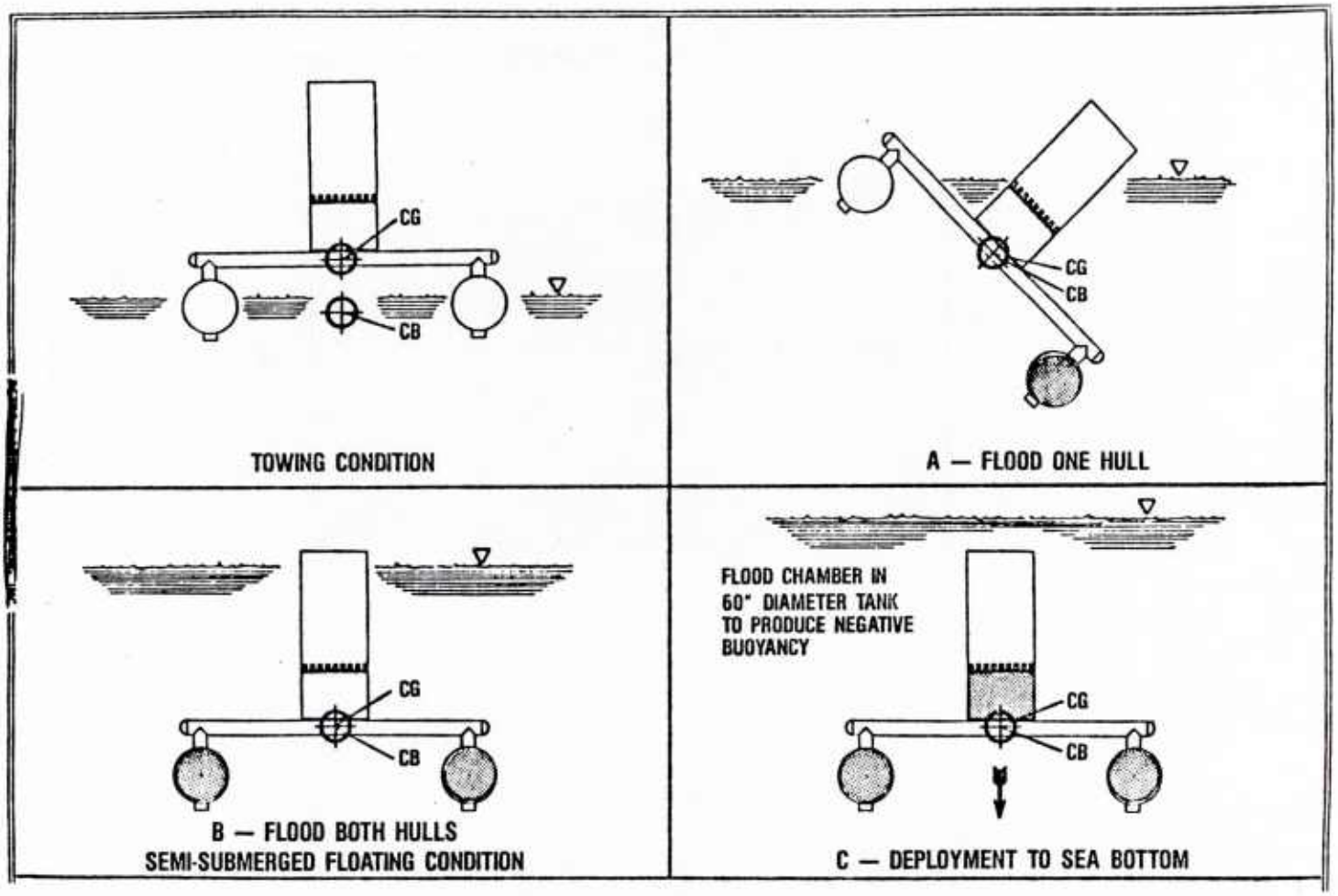

Figure 11. Undersea deployment sequence.

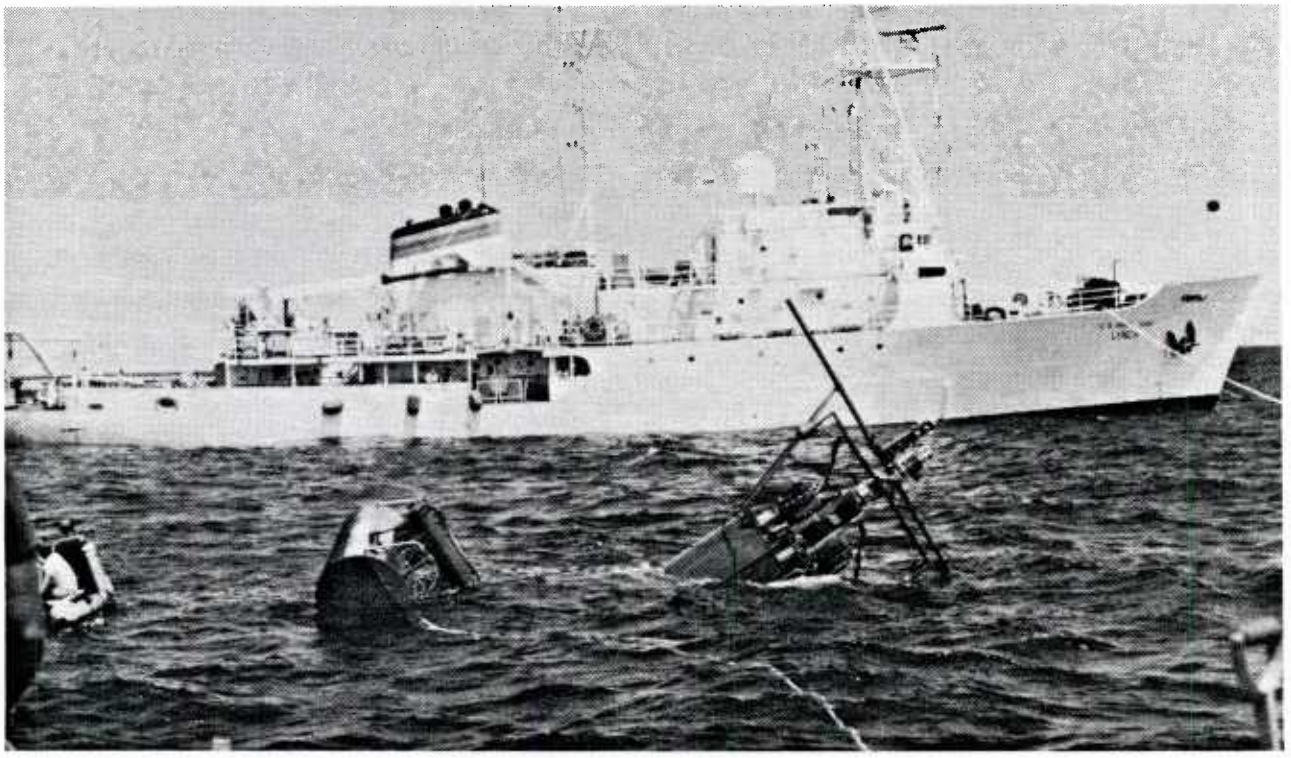

Figure 12. Deployment procedure (one hull flooded).

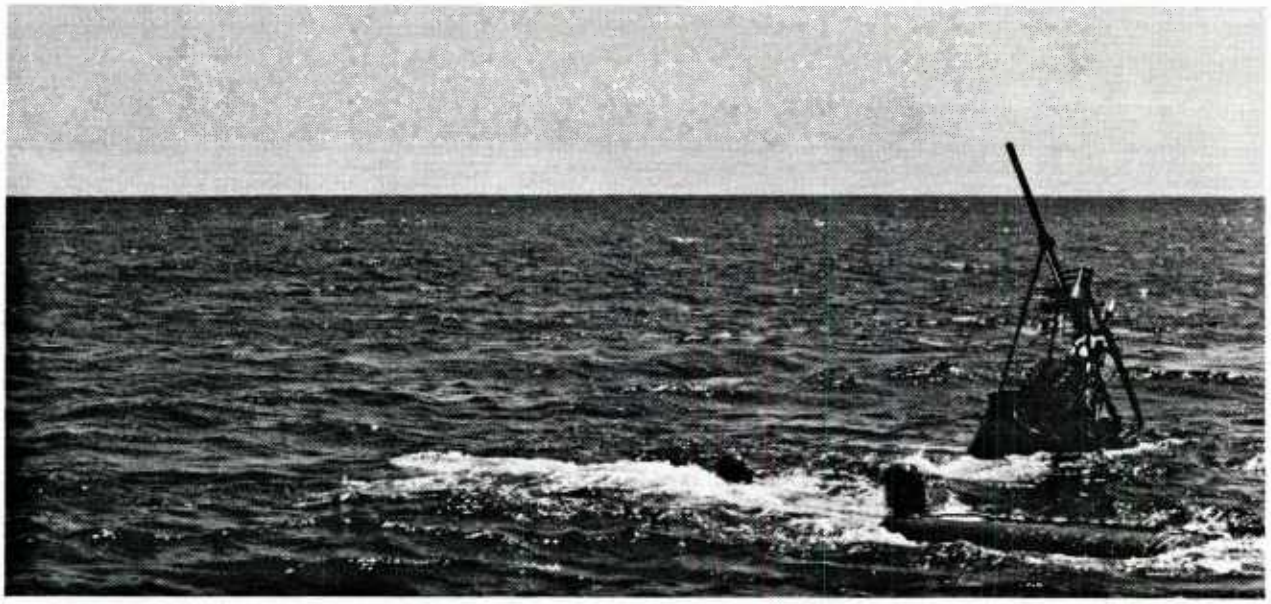

Figure 13. Deployment procedures (second hull flooding).

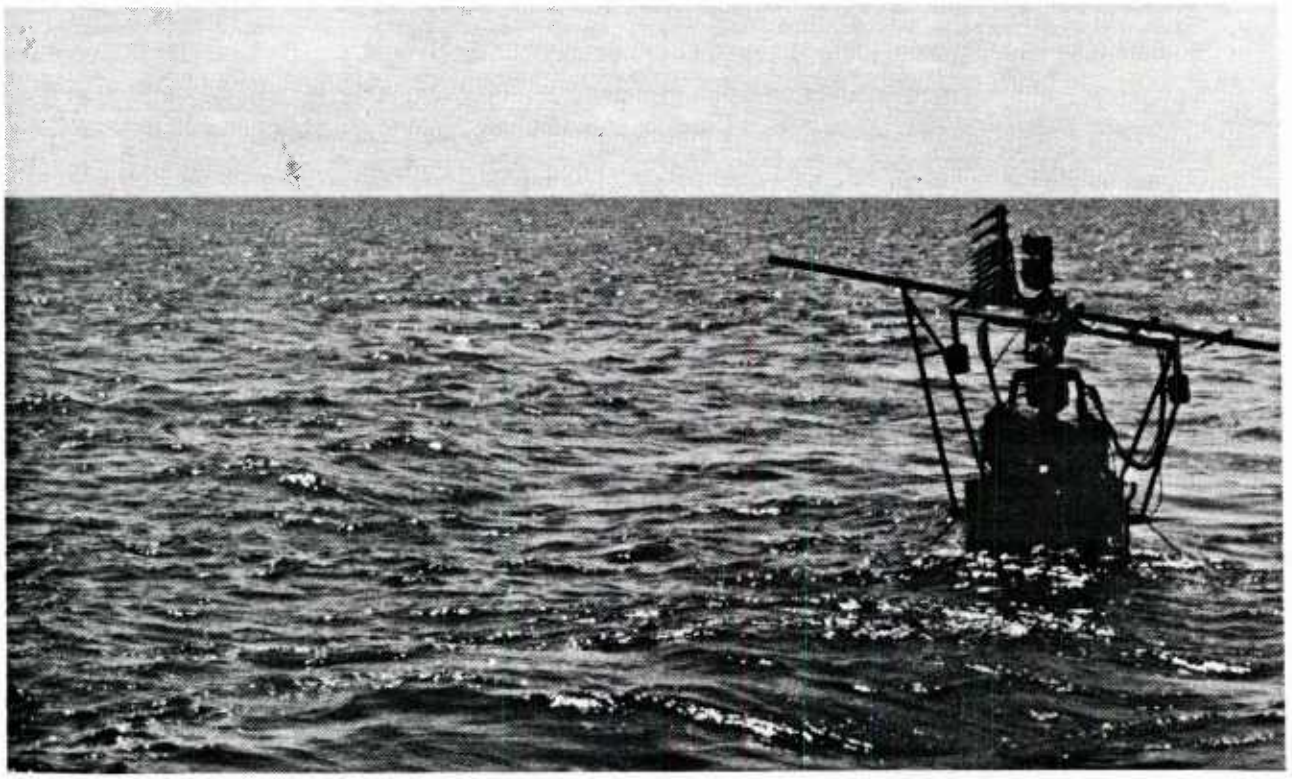

Figure 14. Both hulls flooded (semisubmerged floating condition).

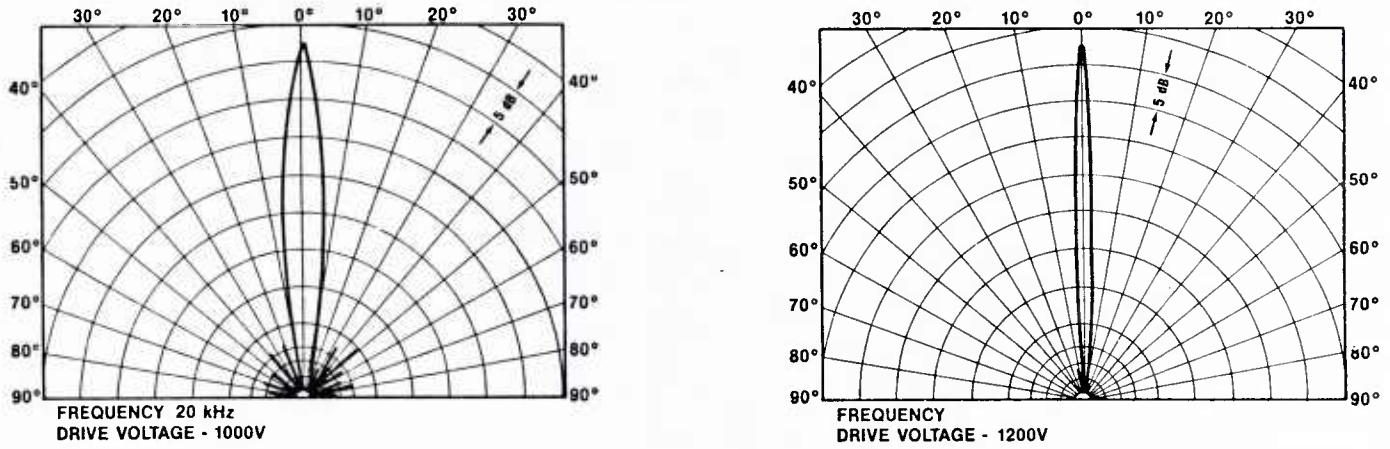

Figure 15. Parametric beam patterns.

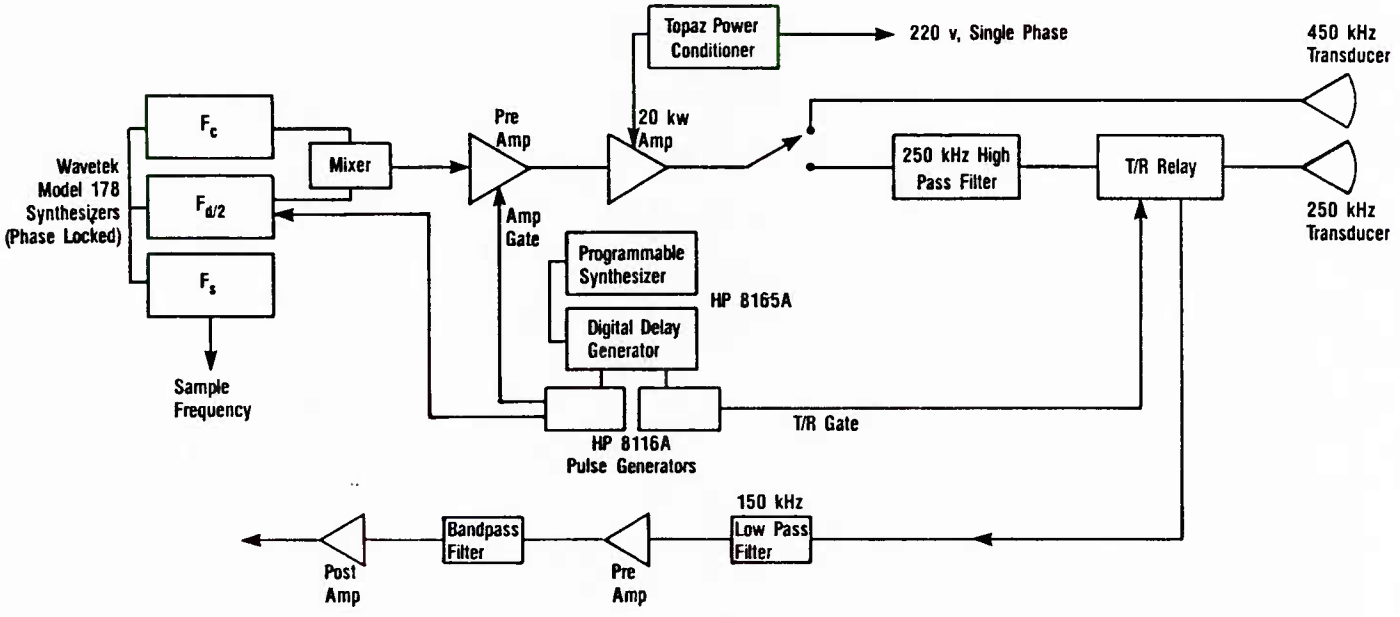

Figure 16. Source transmitting and receiving systems.

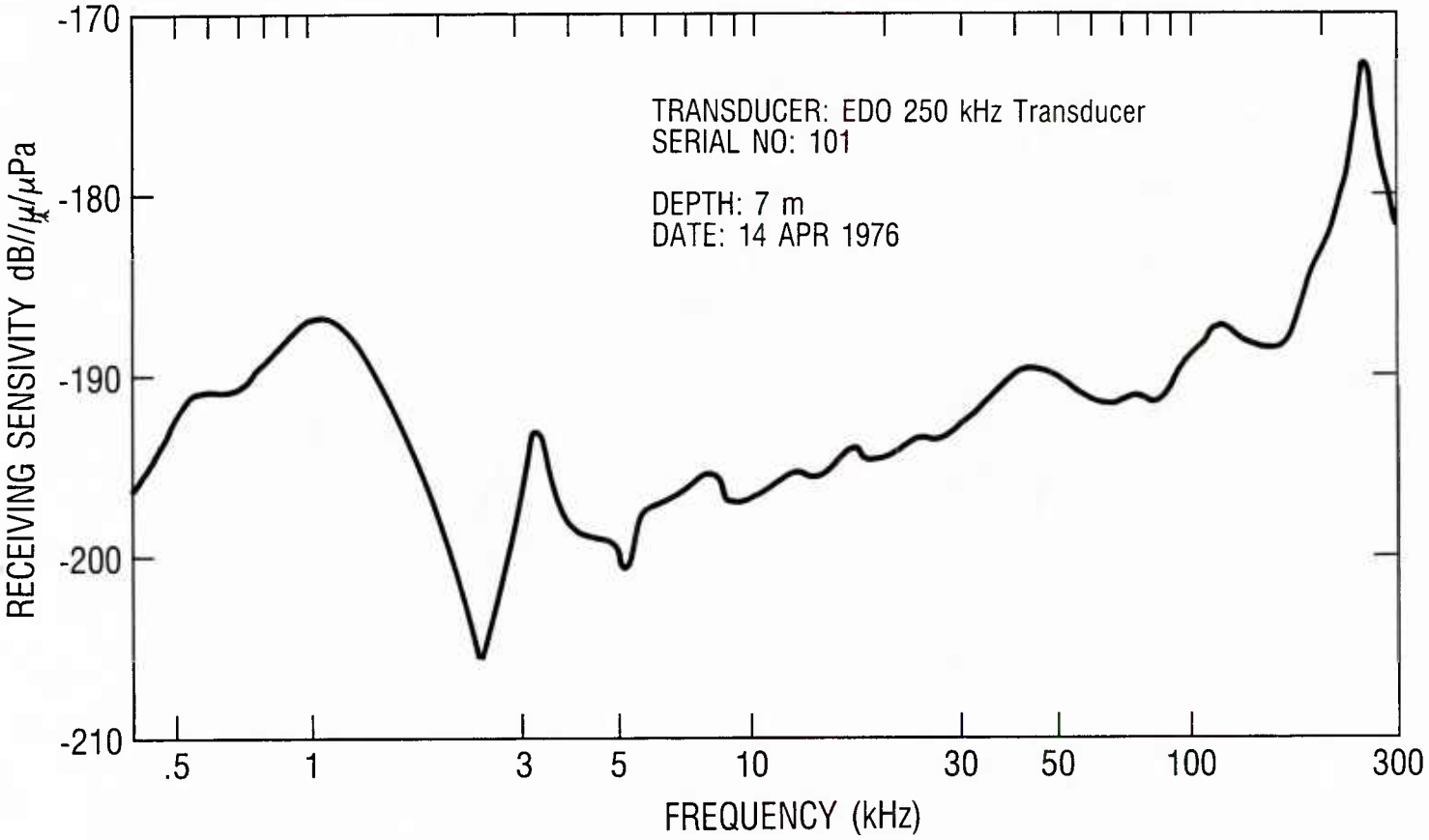

Figure 17. Source receiving sensitivity.

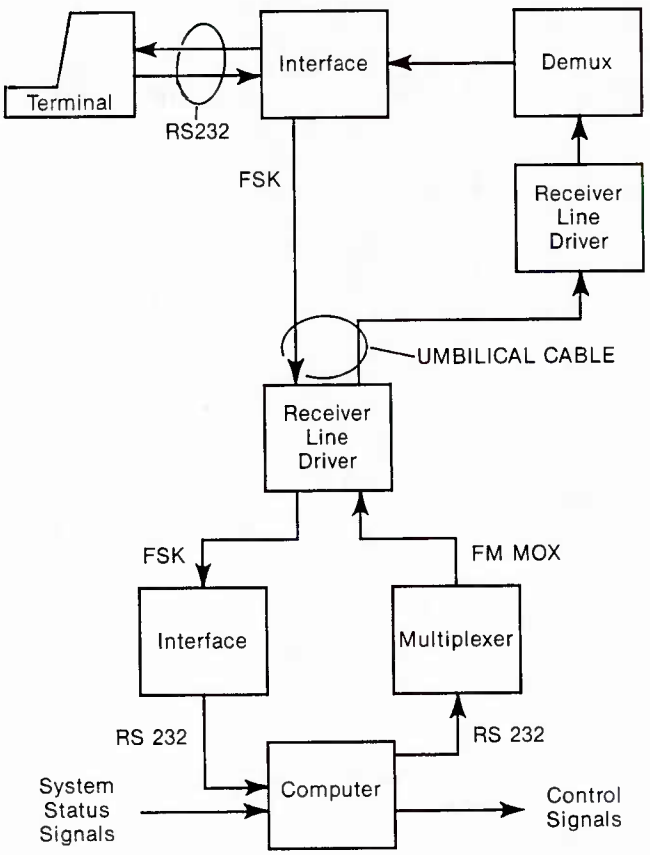

Figure 18. Receiving control system.

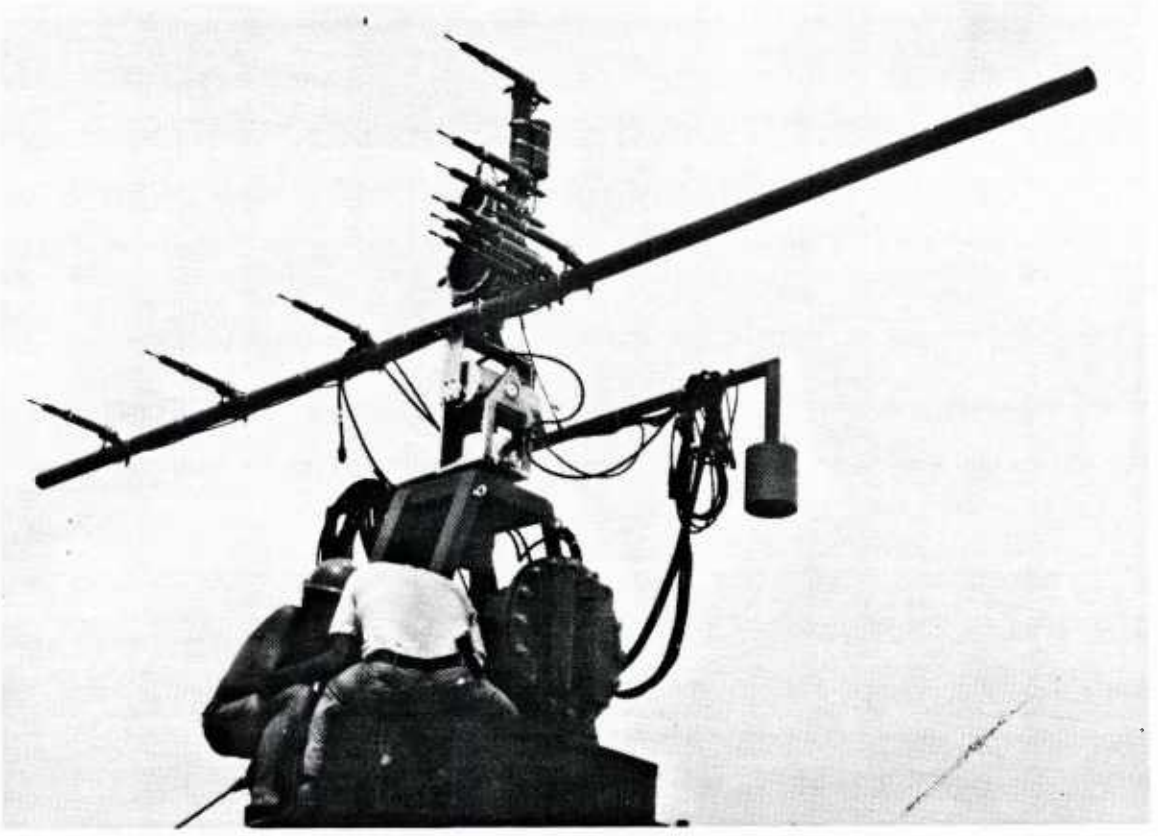

Figure 19. Source/receiving array configuration (Panama City).

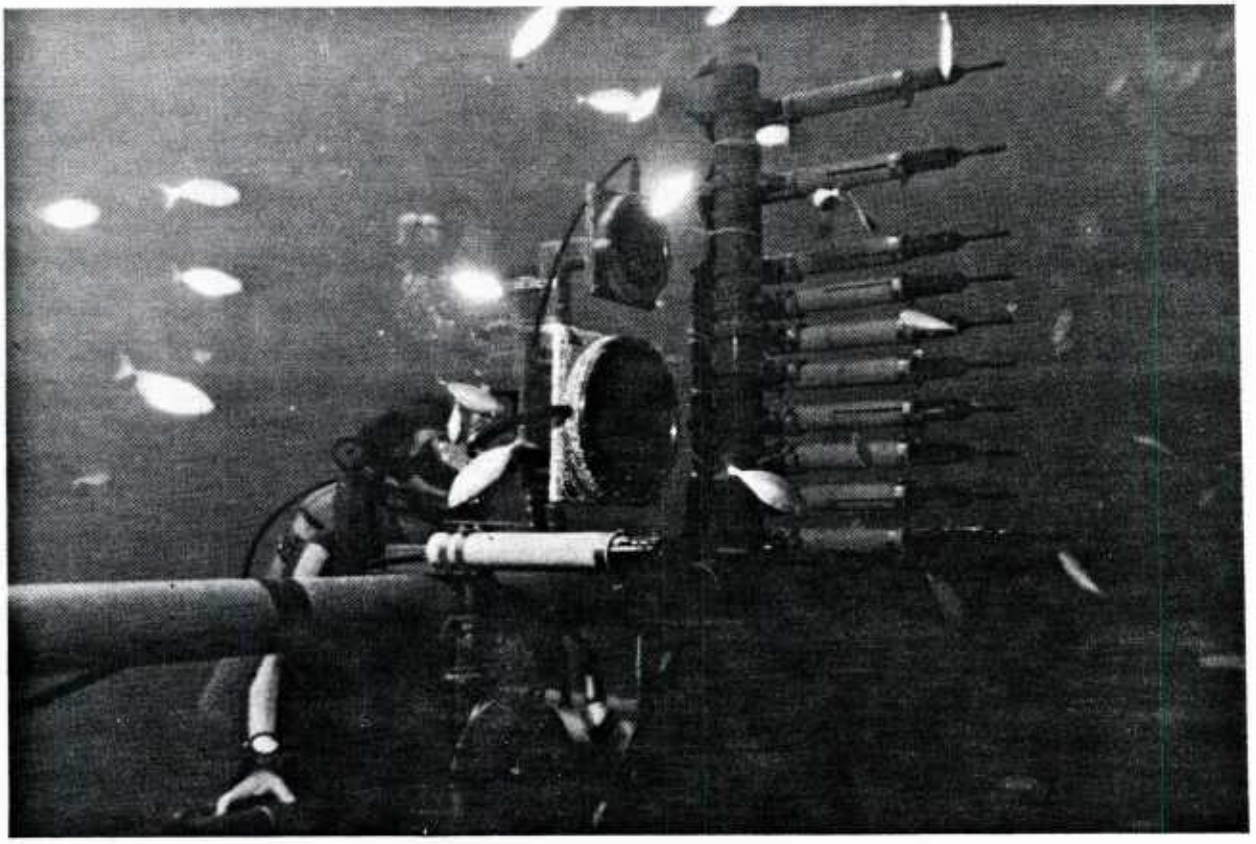

Figure 20. Source/receiving array configuration (Jacksonville).

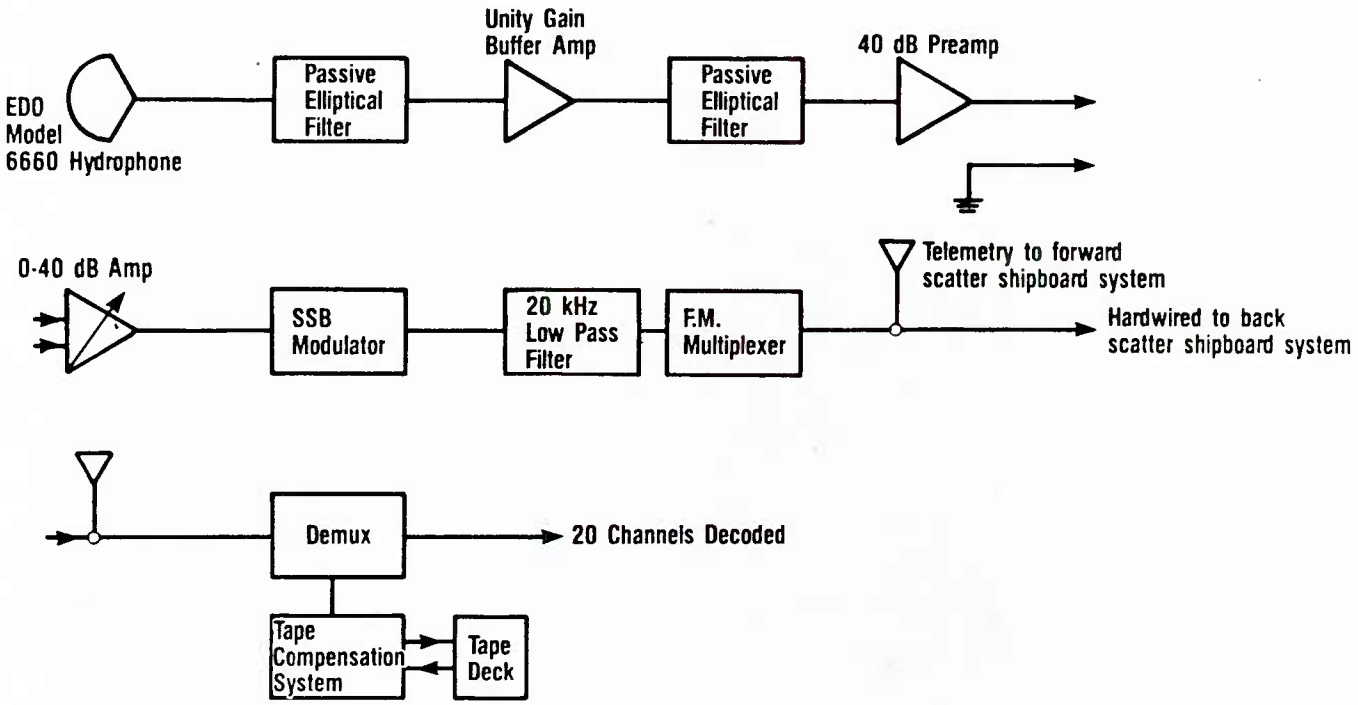

Figure 21. Single-channel configuration.

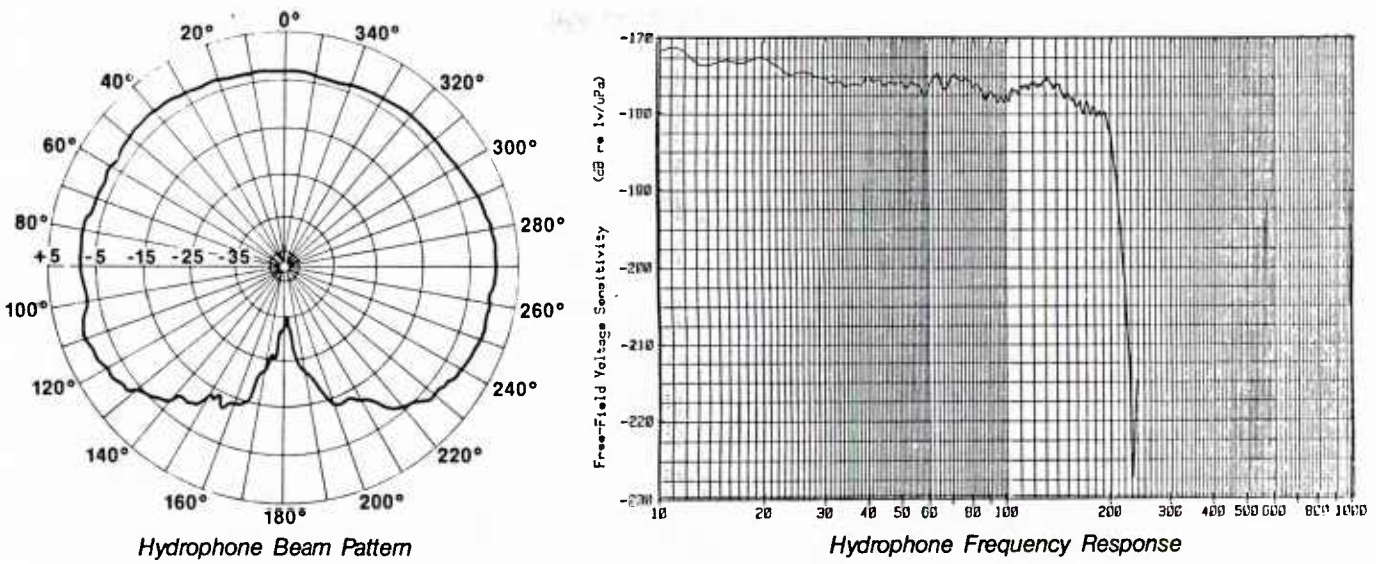

Hydrophone Beam Pattern

Hydrophone Frequency Response

Figure 22. Hydrophone beam pattern and frequency response.

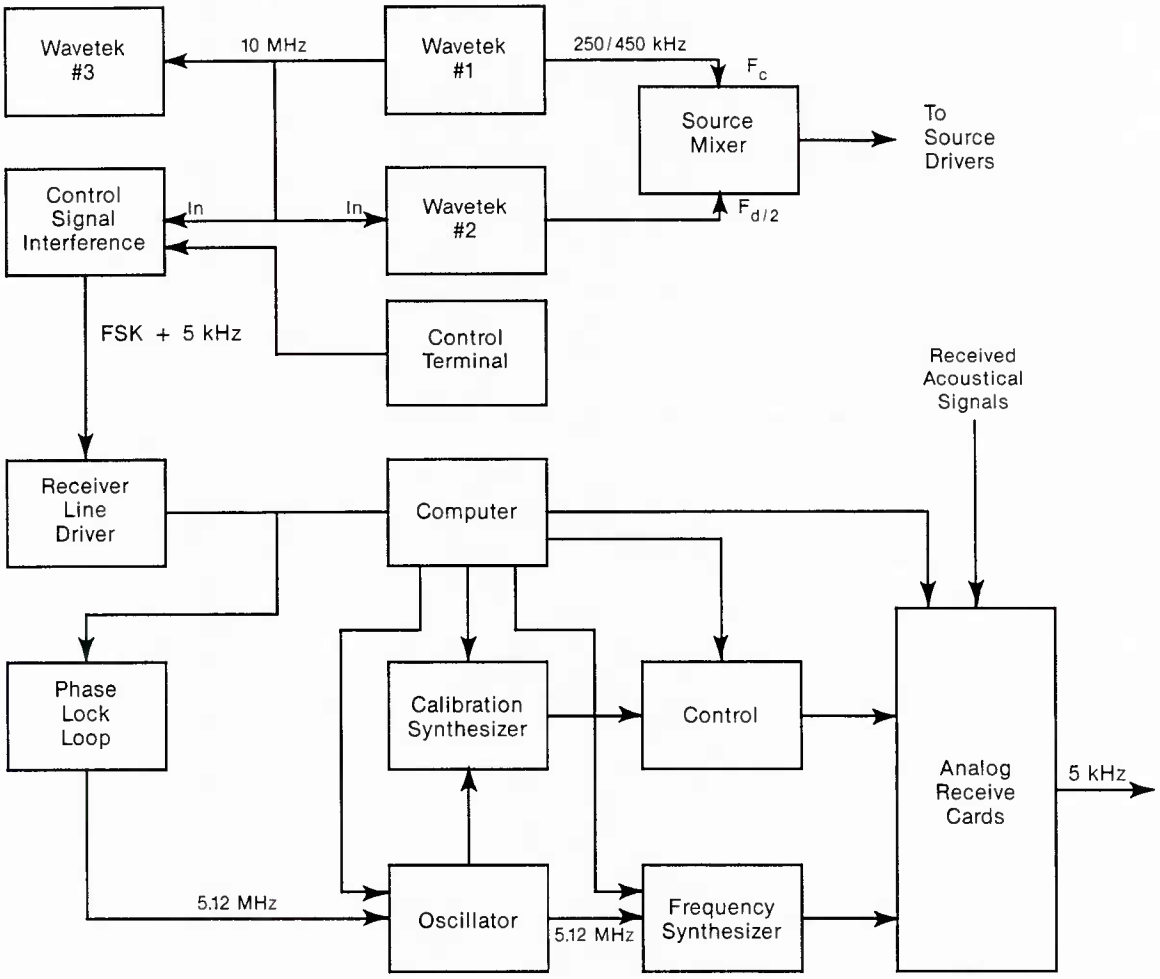

Figure 23. Data acquisition system.

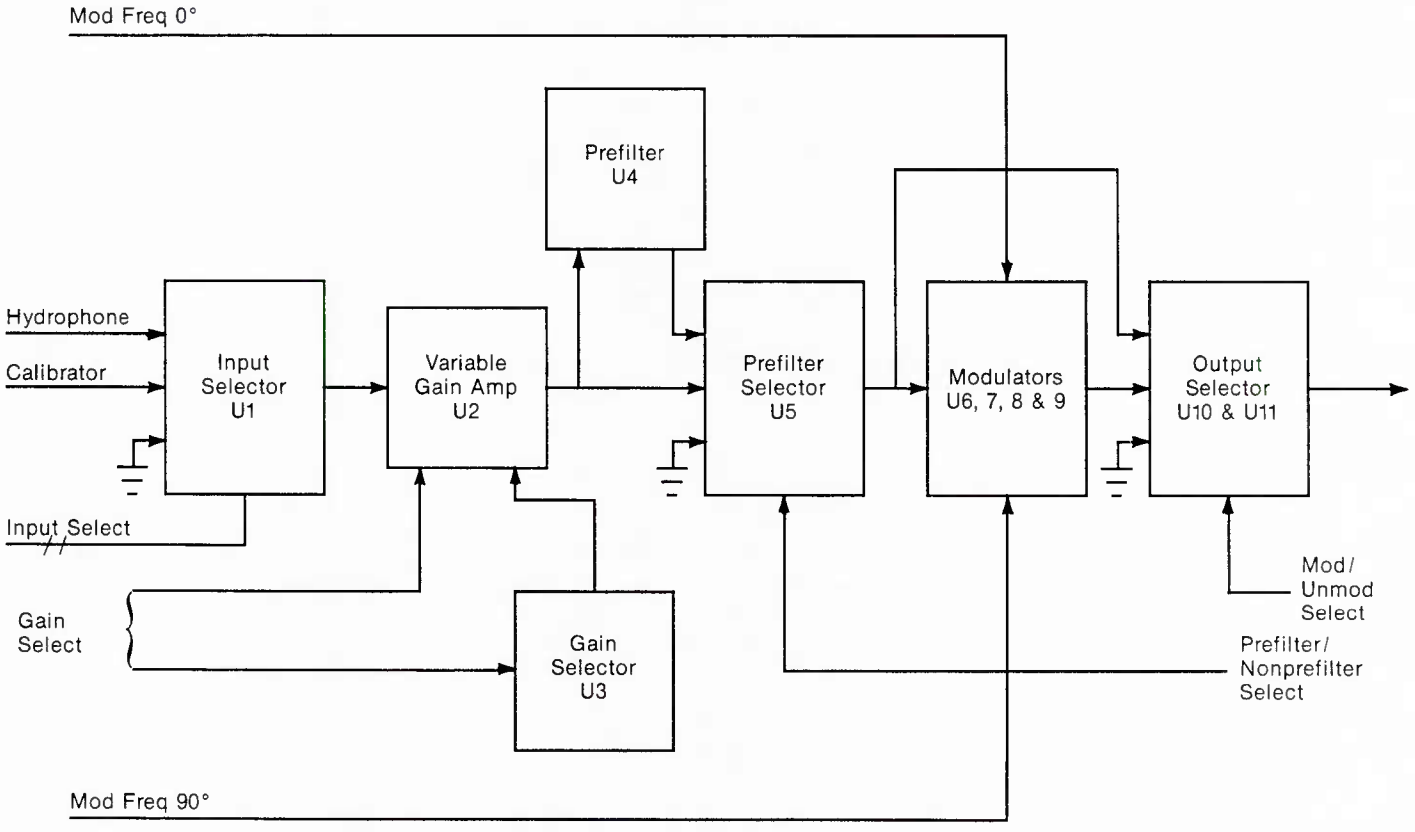

Figure 24. Analog receiver card.

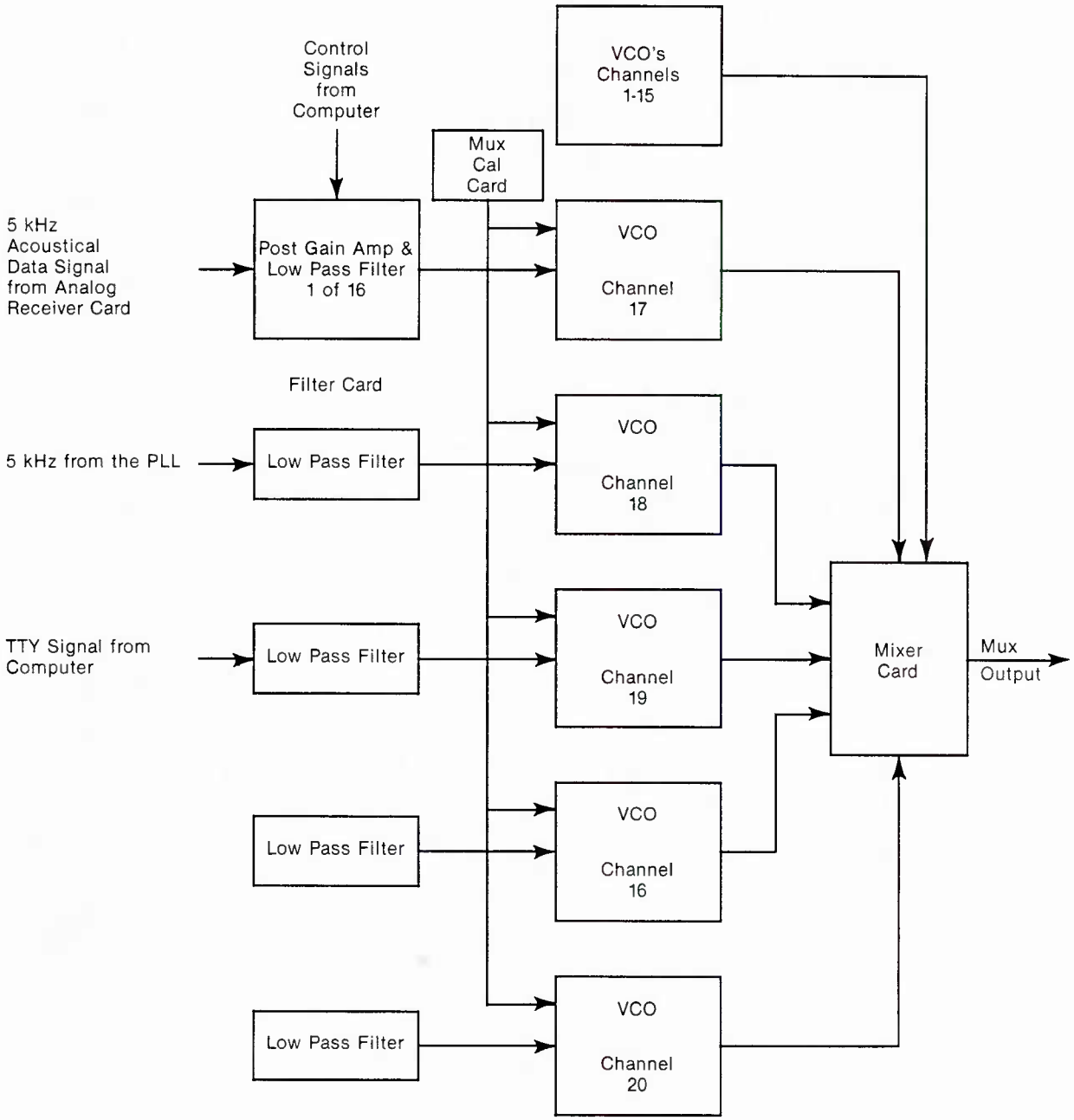

Figure 25. Multiplexing system.

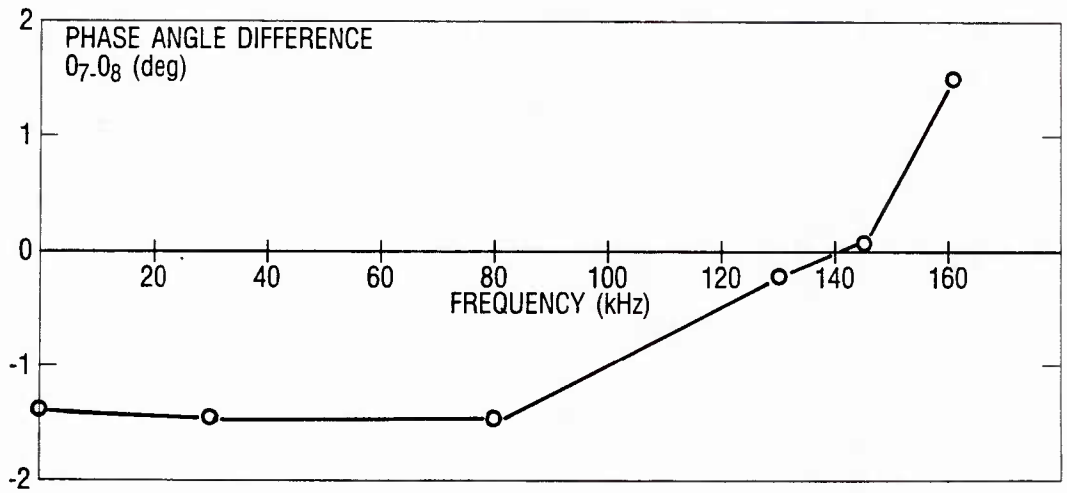

Figure 26. Phase difference between channel 7 and channel 8 forward scatter system.

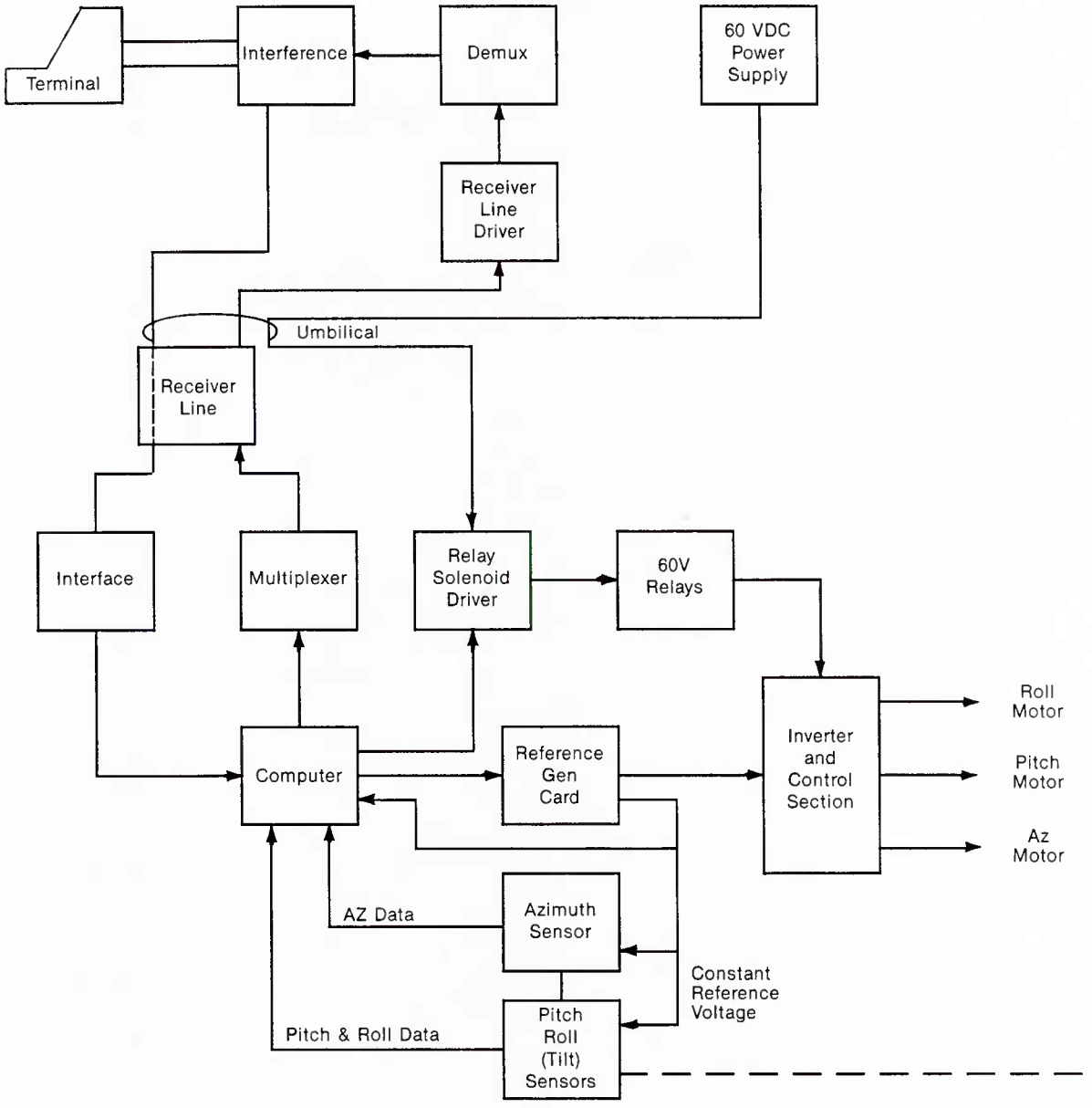

Figure 27. Array control system.

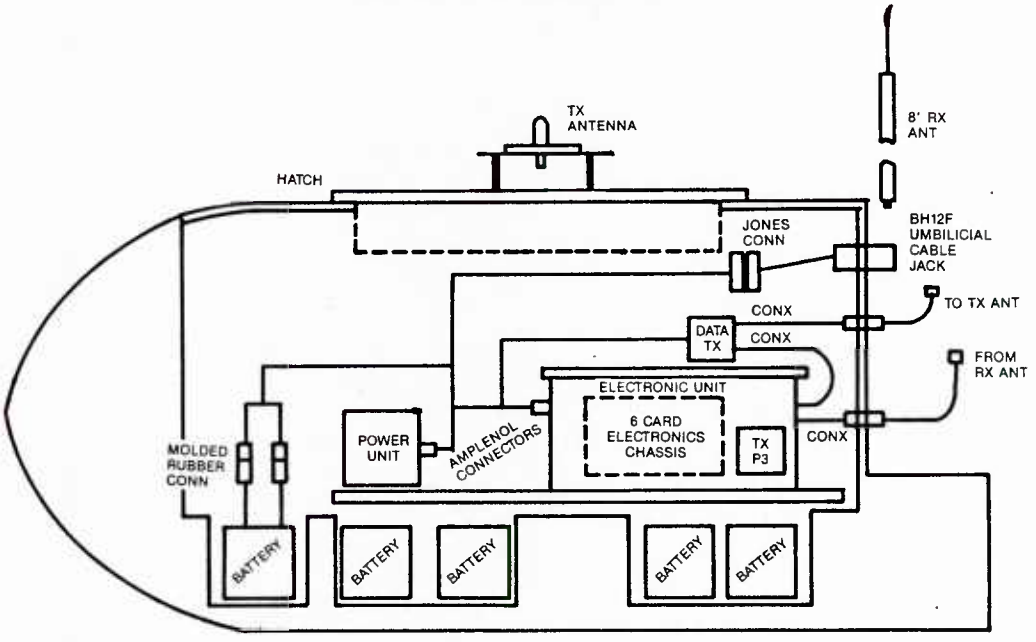

Figure 28. Buoy layout.

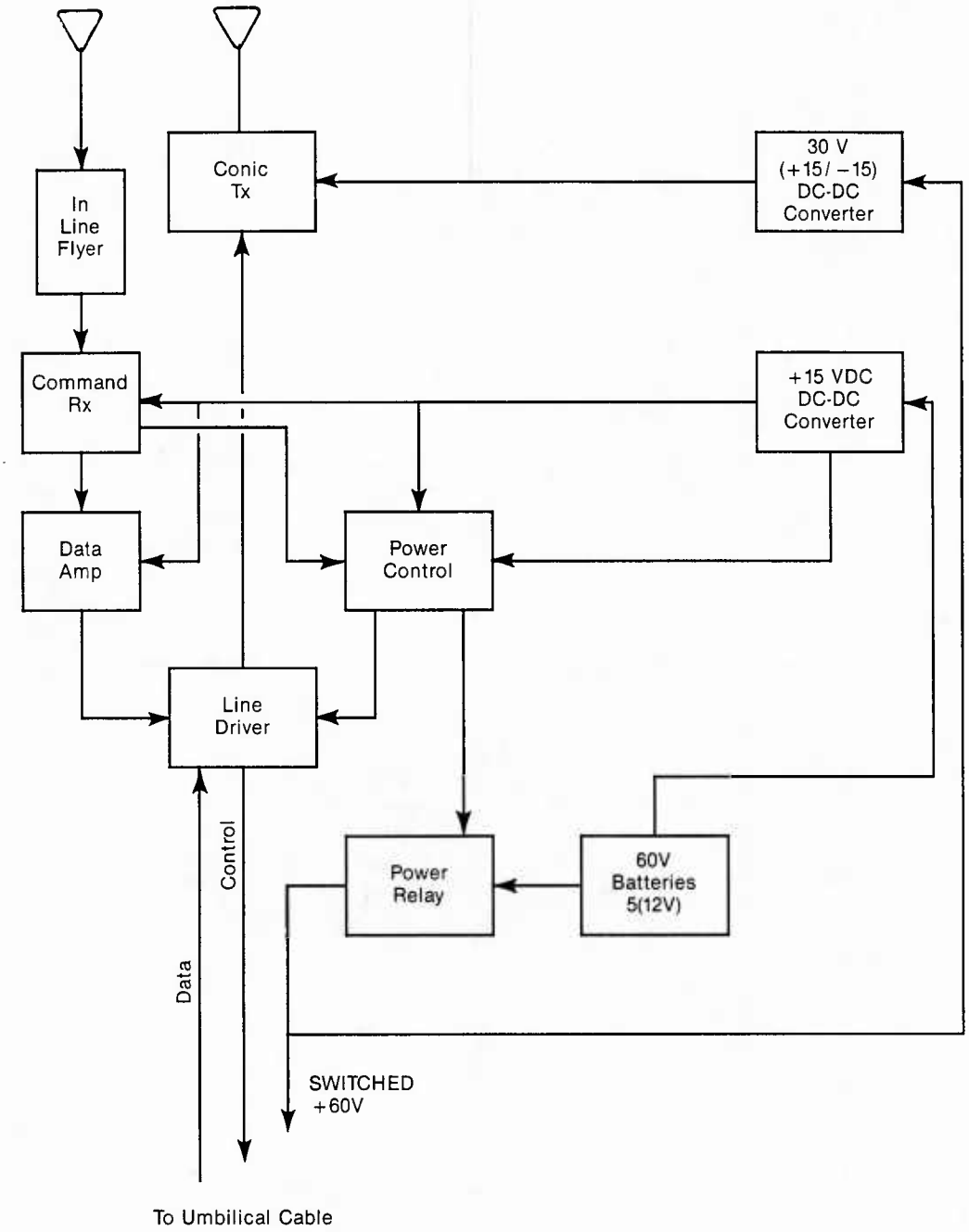

Figure 29. Buoy electronics.

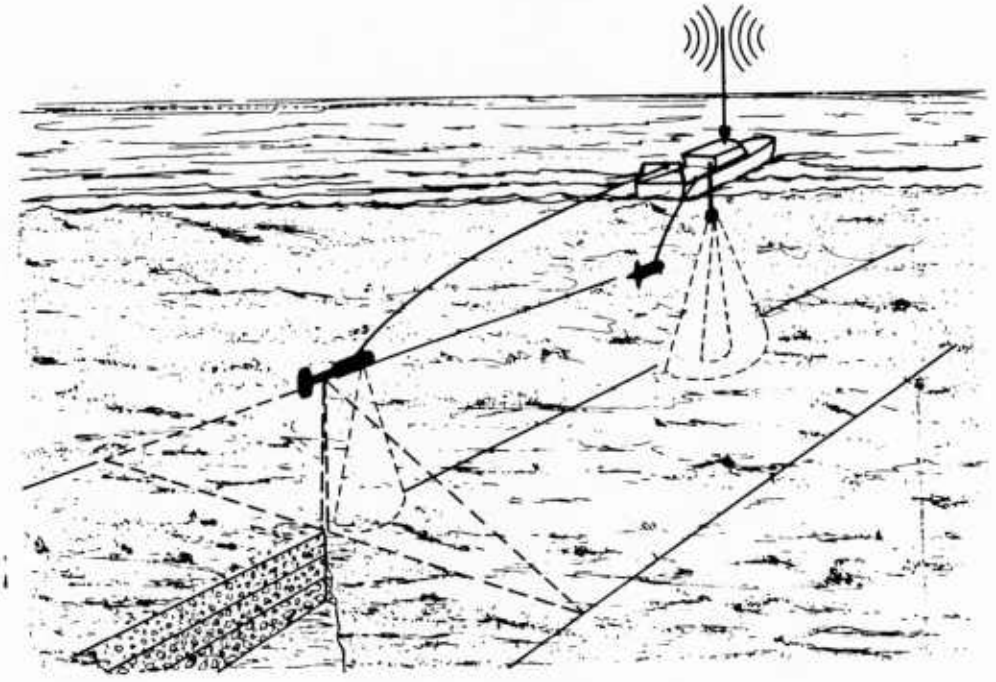

Figure 30. Schematic of sidescan system operation showing sidescan sonar, subbottom profiler, dual-frequency depth sounder, speed sensor, and navigation system.

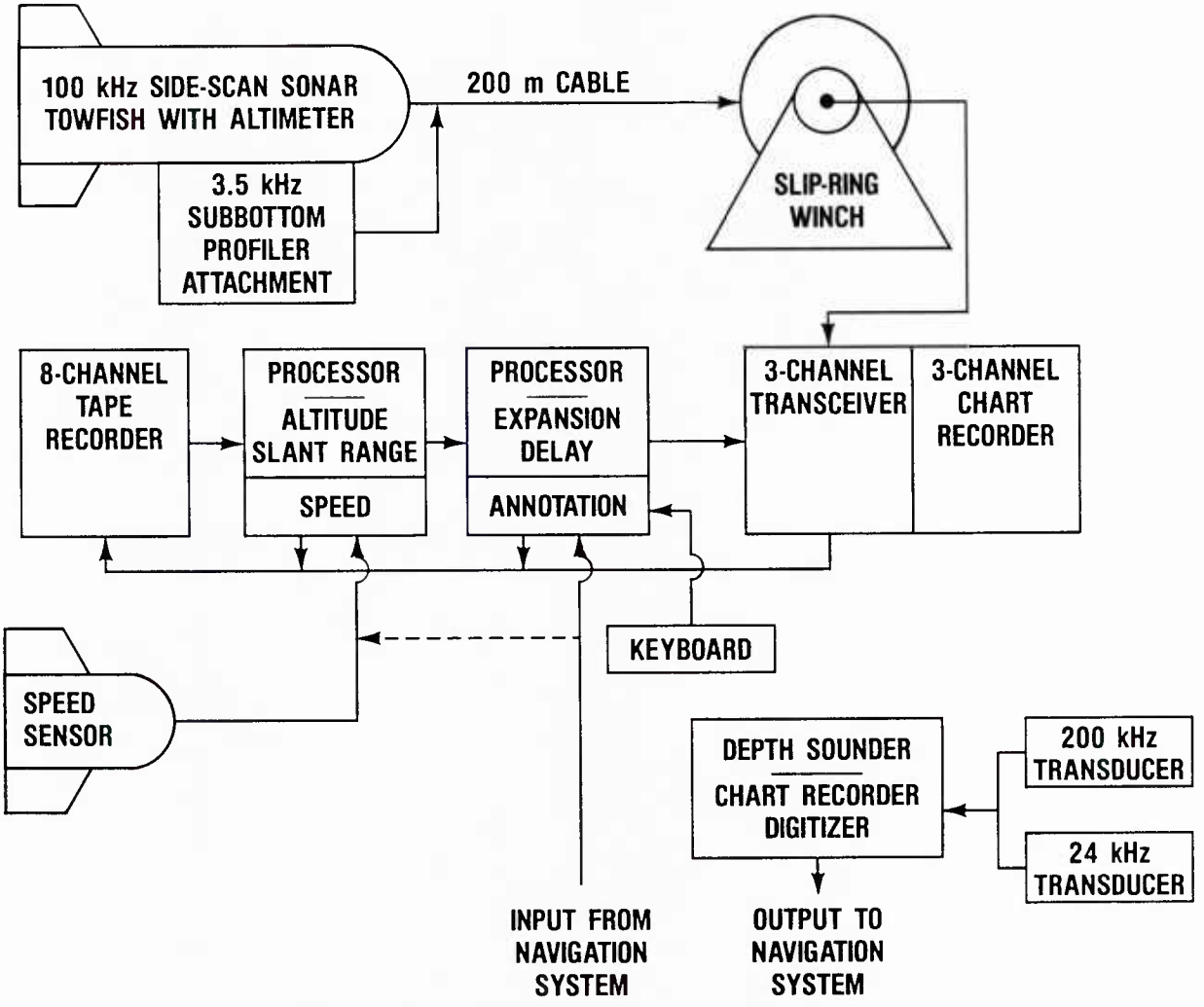

Figure 31. Sidescan sonar measurement system—acoustic components.

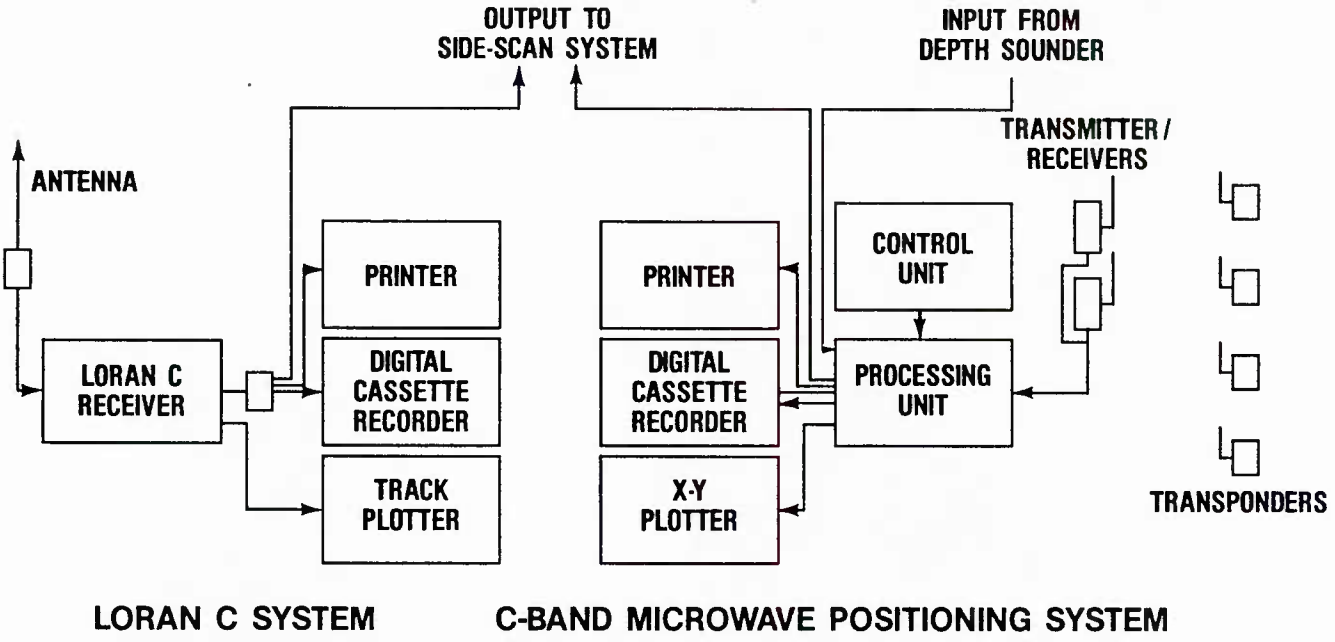

Figure 32. Sidescan sonar measurement system—navigation components.

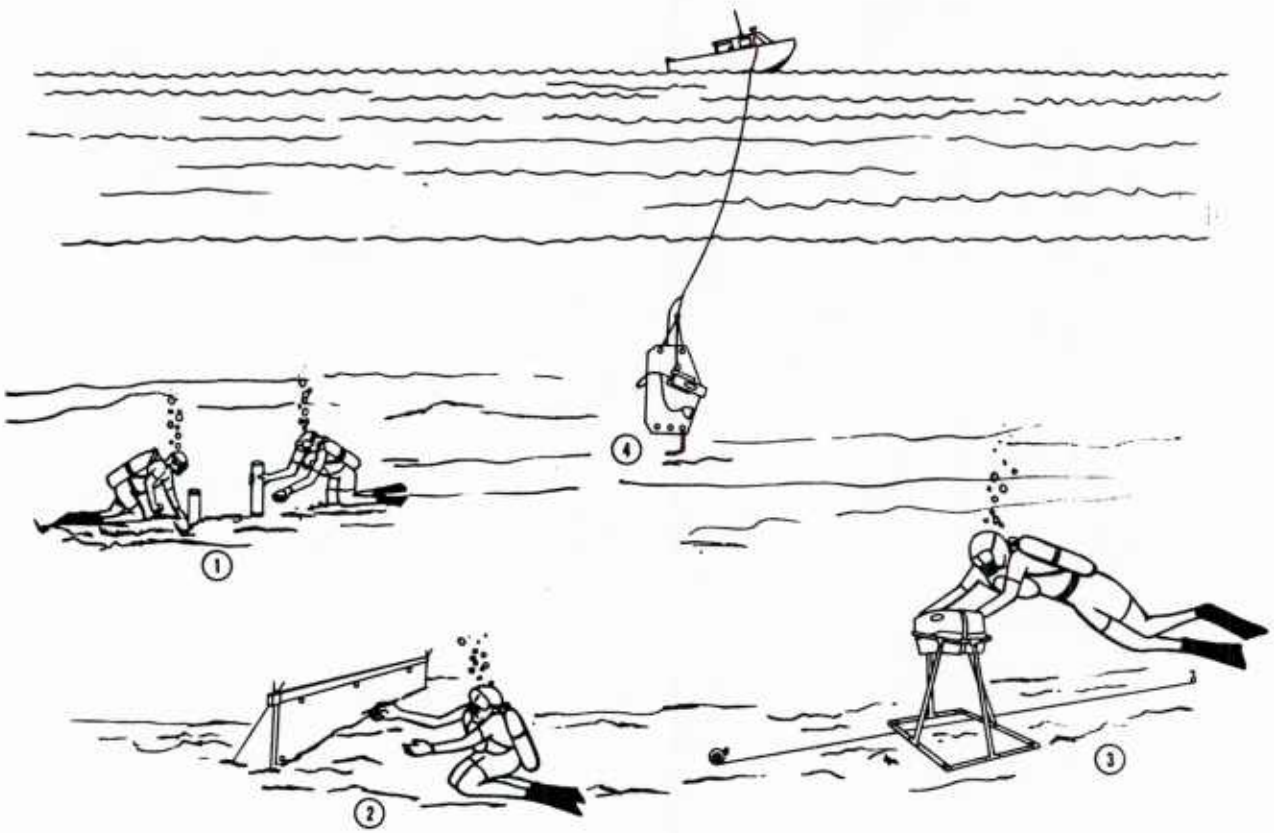

Figure 33. Field collection and characterization by (1) diver-collected cores, (2) manually operated roughness profile apparatus (3) stereo photogrammetric roughness profile apparatus, and (4) vane-mounted video camera.

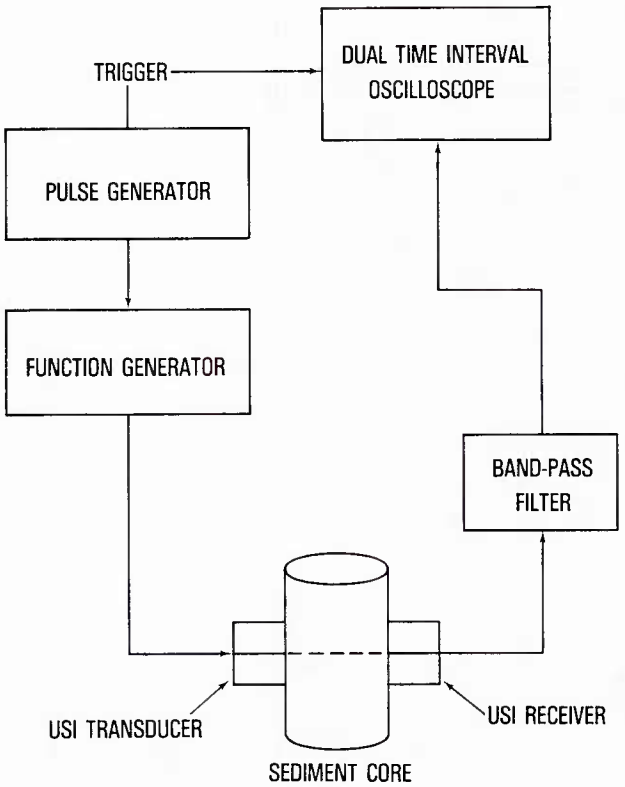

Figure 34. Compressional wave velocity and attenuation measuring system.

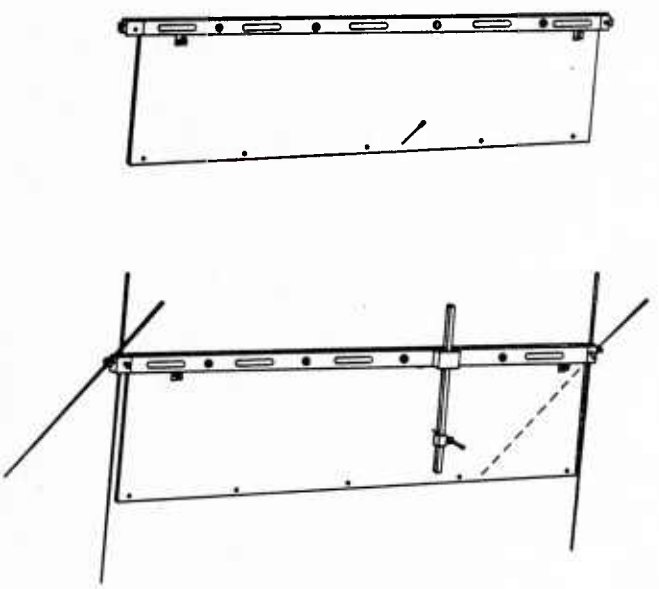

Figure 35. Manual roughness profiling apparatus in two configurations.

Figure 36. Stereophotogrammetric roughness profile apparatus.

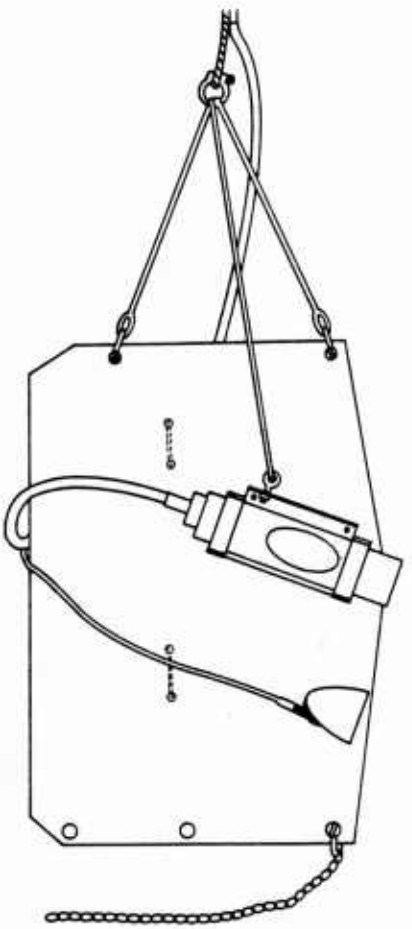

Figure 37. Vane-mounted remote videocamera.

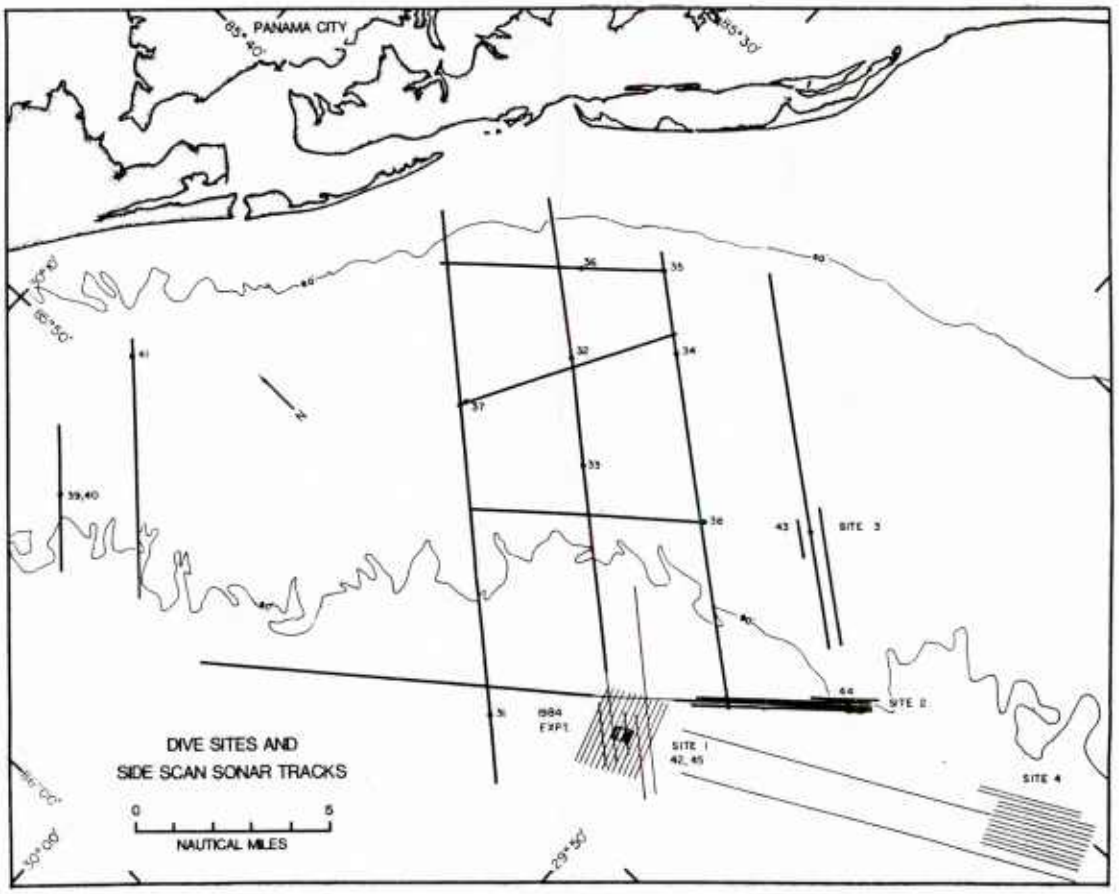

Figure 38. Experimental areas off Panama City. First experiment was site 1, proposed experiment location is site 4.

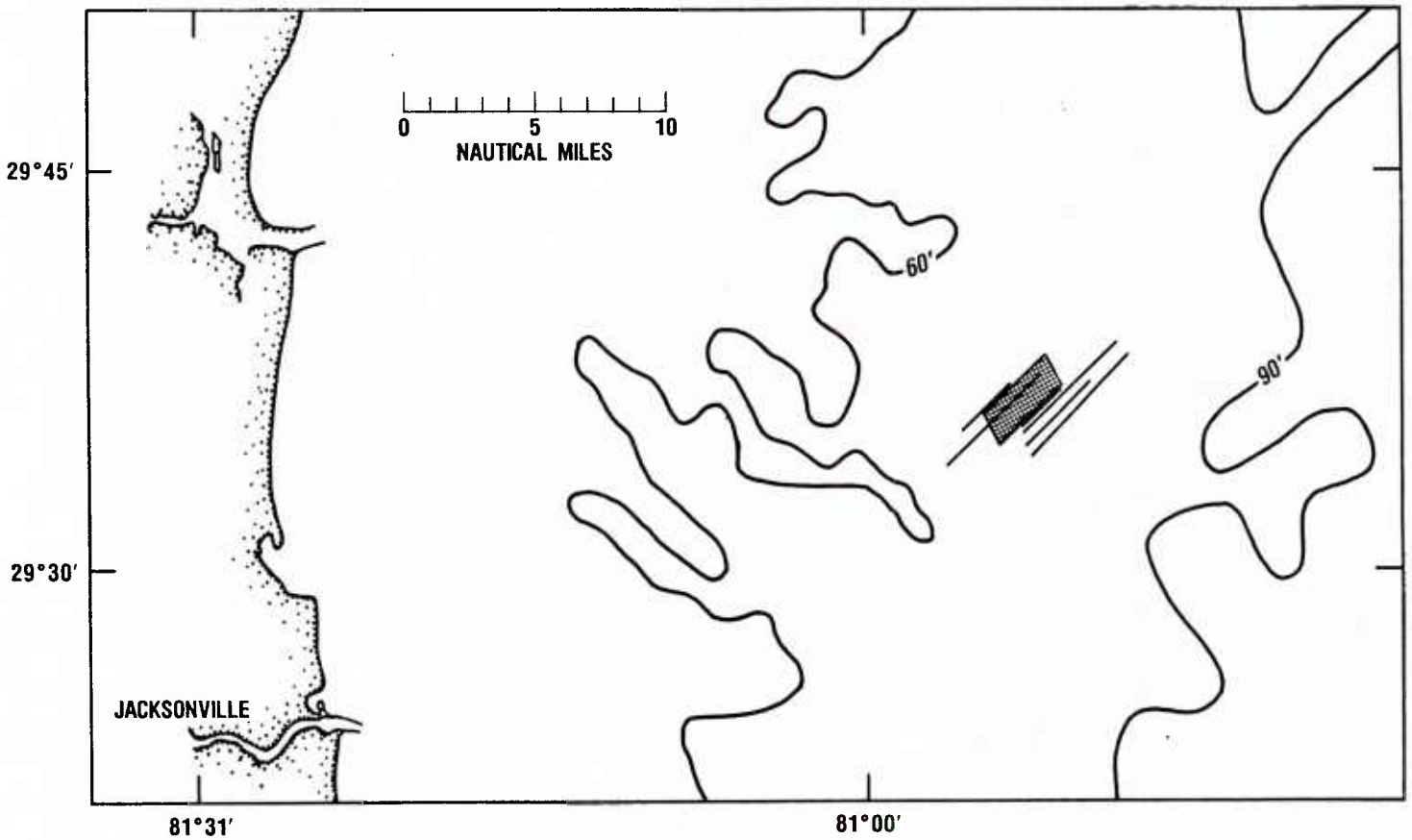

Figure 39. Area of second experiment, off Jacksonville.

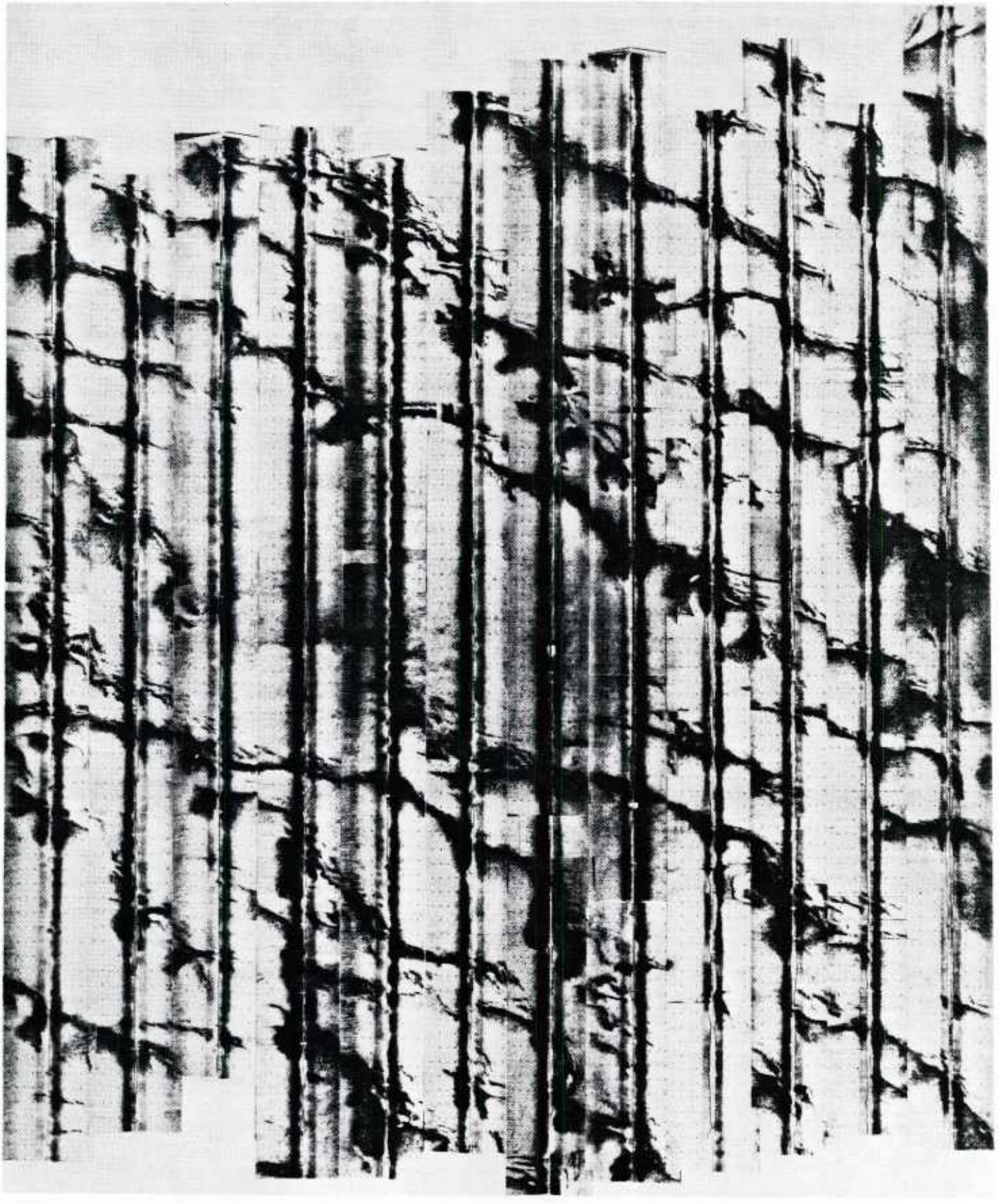

Figure 40. Sidescan mosaic of Panama City site, showing the uniform, featureless, and level experiment site (center) and surrounding sand ridges. North is toward the upper left corner and scale is indicated by the 25-m tick-mark spacing on the mosaic. See Fig. 38 for trackline locations.

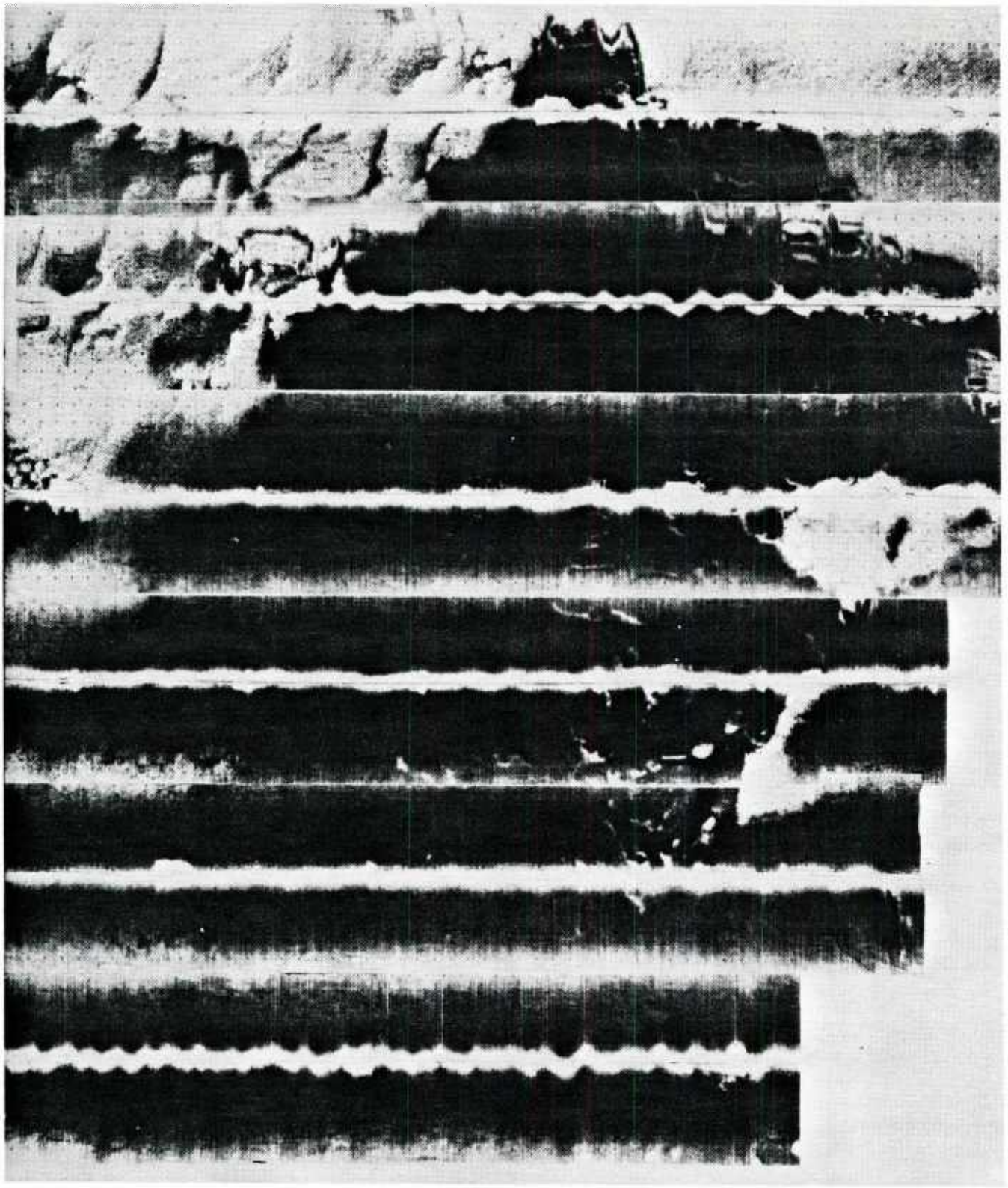

Figure 41. Sidescan mosaic of Jacksonville site. The experiment site is located within the center of the uniformly dark area (coarse shell hash). Tracklines are aligned SW (left)–NE (right), and tick-marks are on a 25-m spacing. The mosaic is located within the shaded area of Fig. 39.

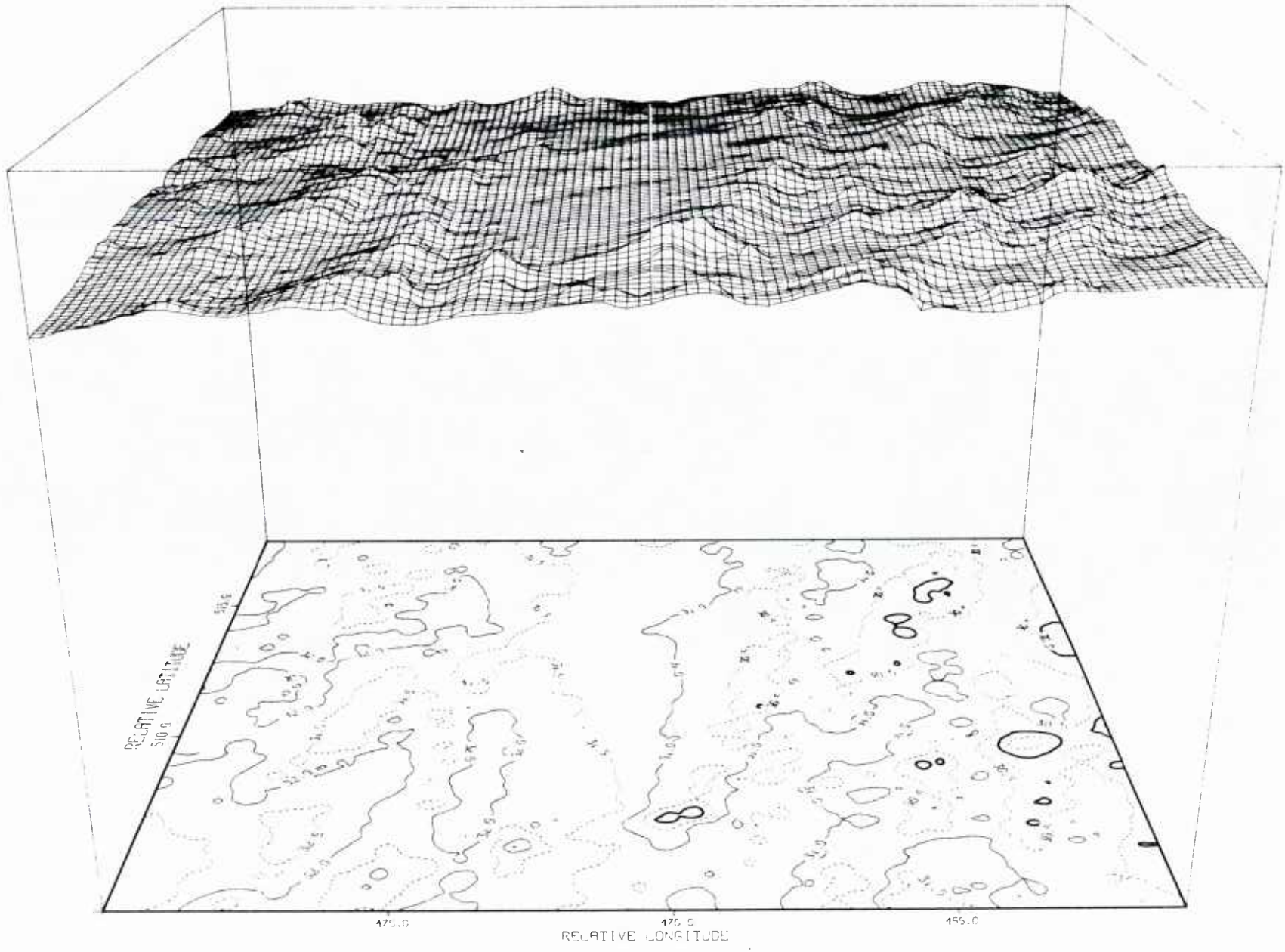

Figure 42. Bathymetric map and projection of Panama City site and environs. The site is the flat circular area in the projection. Contour interval is 0.5 m.

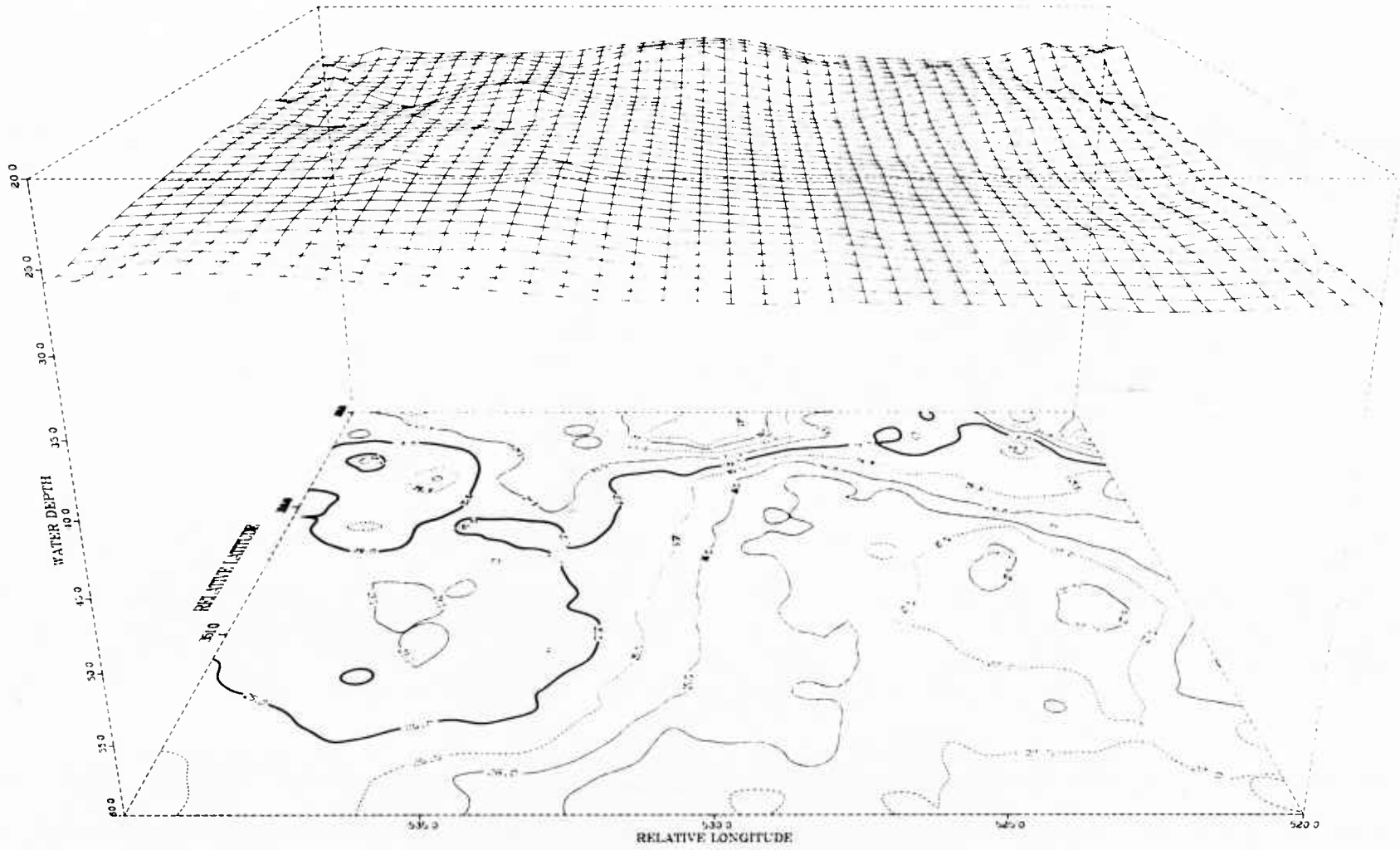

Figure 43. Bathymetric map and projection of Jacksonville site and environs. The site is approximately in the center of the map. Contour interval is 0.5 m.

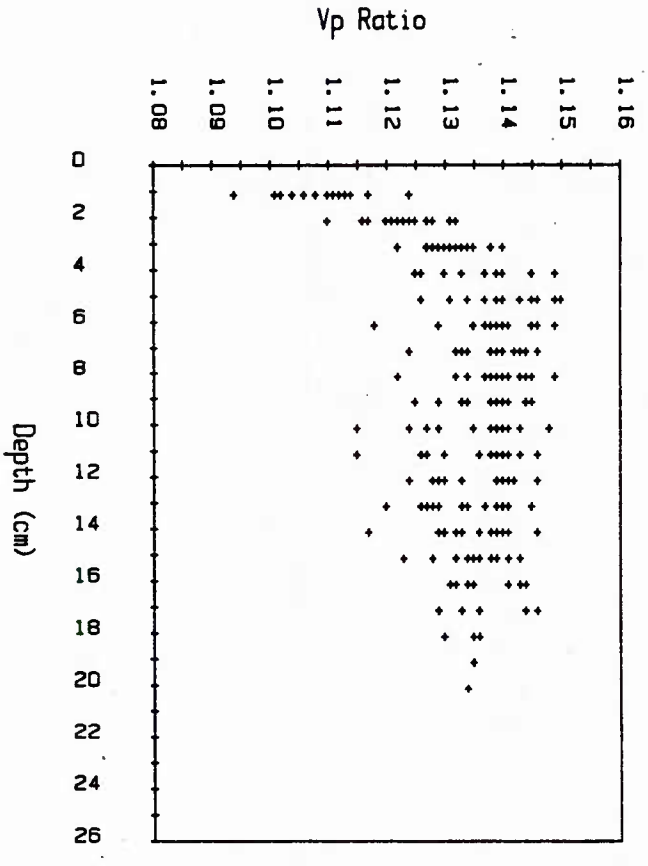

Figure 44. Vertical distribution of sediment compressional wave velocity ratio (Vp ratio) obtained from 15 cores collected at the Panama City experiment site in August–September 1984.

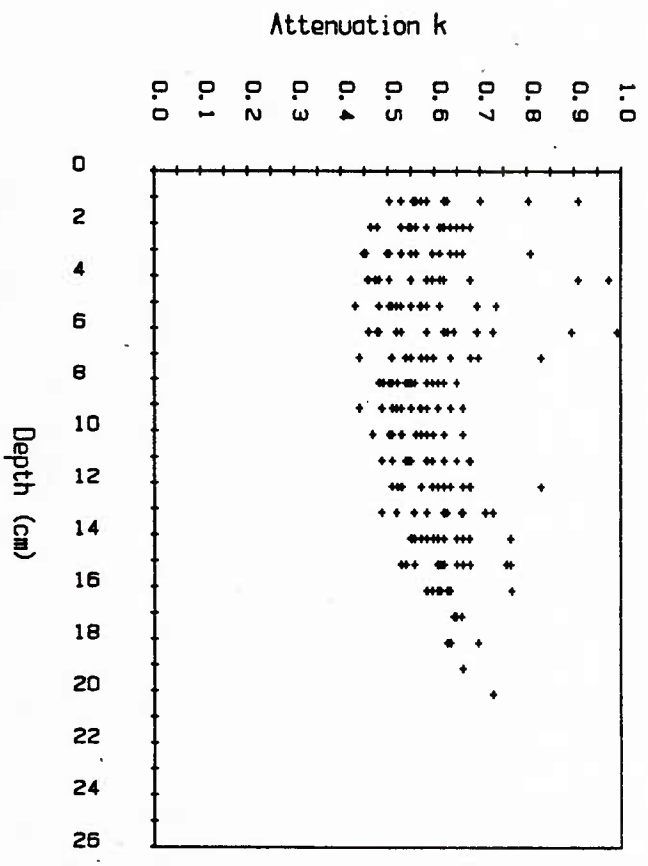

Figure 45. Vertical distribution of sediment compressional wave attenuation (k) obtained from 15 cores collected at the Panama City experiment site in August–September 1984.

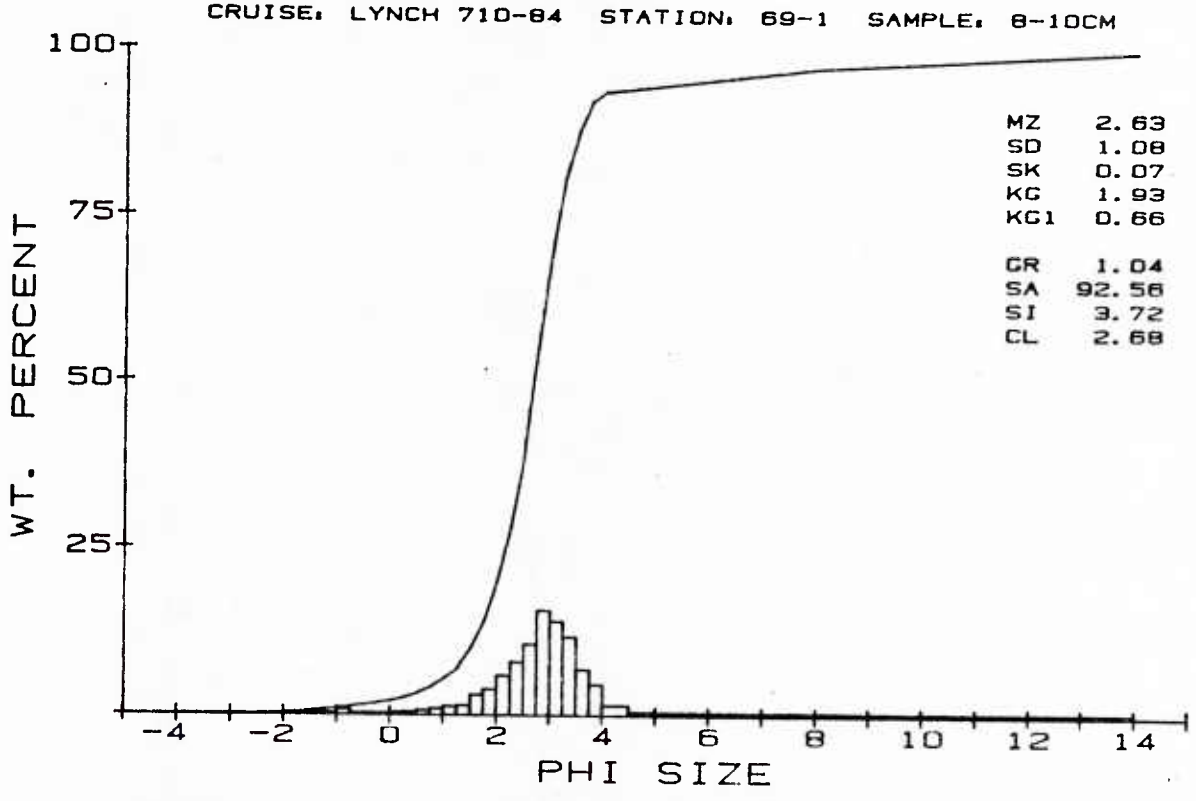

Figure 46. Grain-size data plotted as weight-percent histograms and cumulative weight curve. Gravel and sand fractions are divided into 1/4 ϕ intervals, silt fraction is divided in 1/2 ϕ intervals, and clay fraction is divided in 1 ϕ intervals.

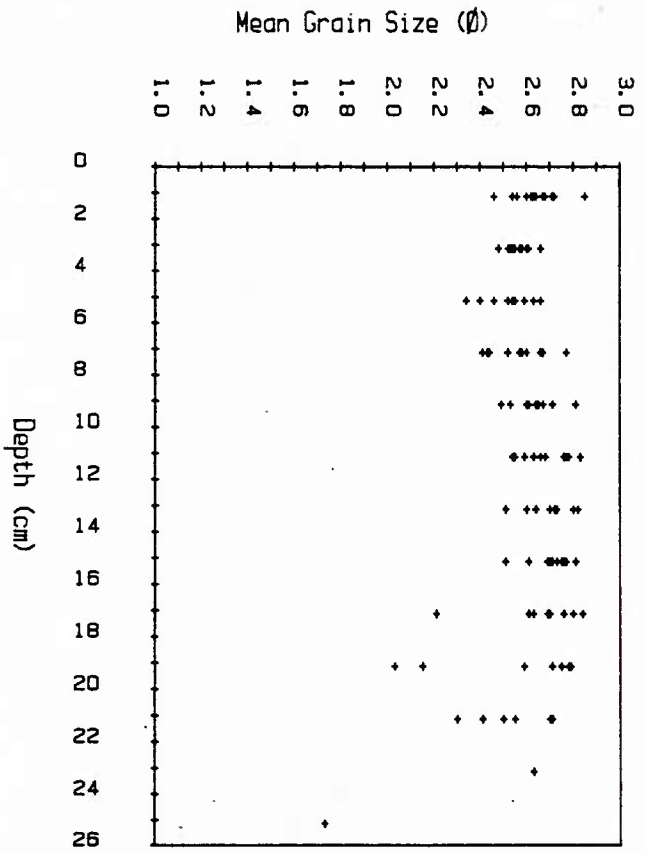

Figure 47. Vertical distribution of mean grain size (ϕ) obtained obtained from 15 cores collected at the Panama City experiment site in August-September 1984.

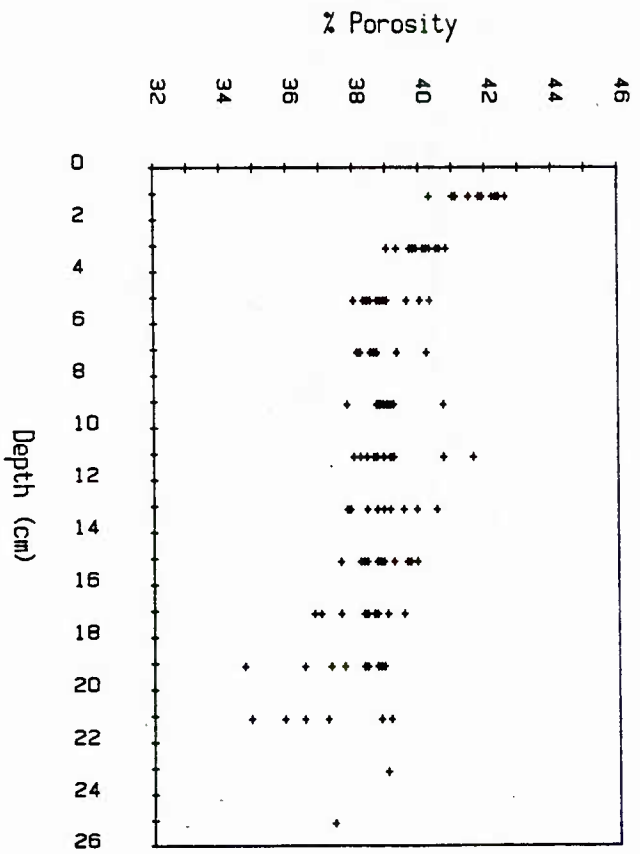

Figure 48. Vertical distribution of sediment porosity (%) obtained from 15 cores collected at the Panama City experiment site in August-September 1984.

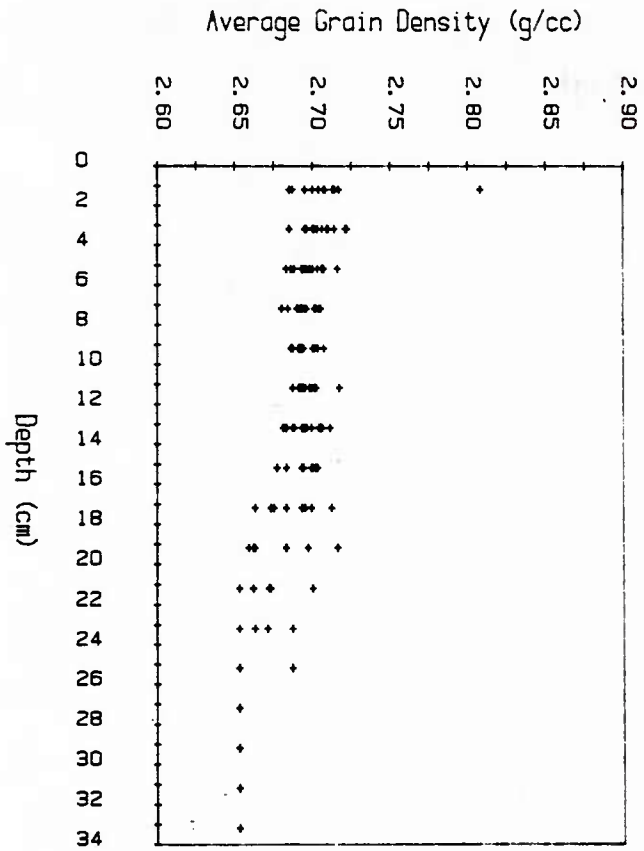

Figure 49. Vertical distribution of average sediment density (g/cm³) obtained from 15 cores collected at the Jacksonville experiment site in August 1985.

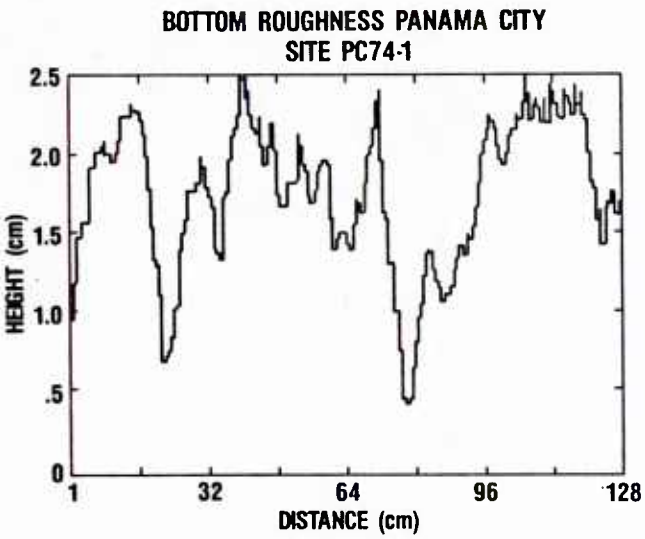

Figure 50. Representative height profile from a bottom trace of the Panama City experiment site. Vertical dimension is exaggerated compared to horizontal dimension.

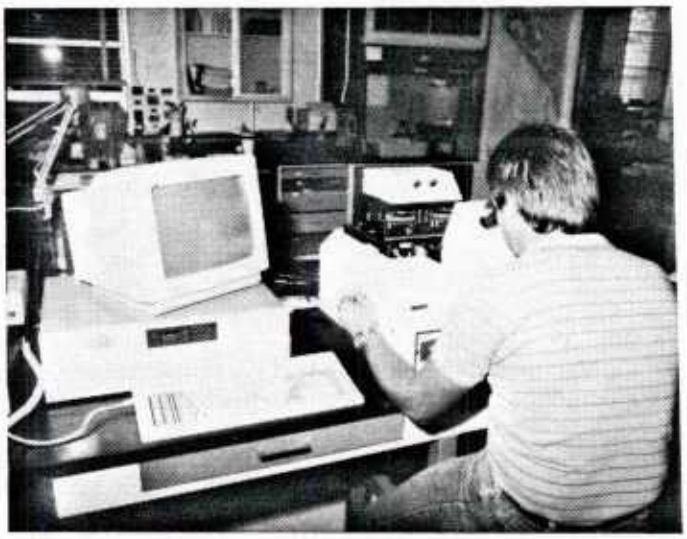

Figure 51. Operator seated at Seagle 90 subsea photogrammetric comparator in the act of digitizing a stereophotograph for roughness profiles. Zenith 248 microcomputer is on the left.

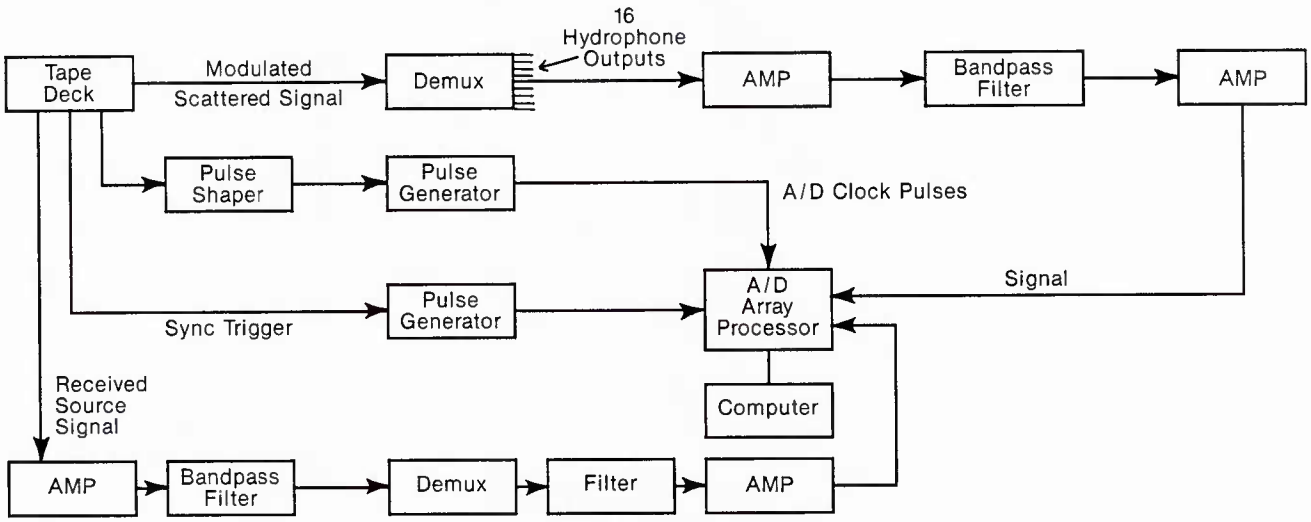

Figure 52. Playback/processing system.